

Multidomain, Surface Layer-associated Glycoside Hydrolases Contribute to Plant Polysaccharide Degradation by *Caldicellulosiruptor* Species^{*[5]}

Received for publication, December 15, 2015, and in revised form, January 25, 2016. Published, JBC Papers in Press, January 26, 2016, DOI 10.1074/jbc.M115.707810

Jonathan M. Conway¹, William S. Pierce, Jaycee H. Le, George W. Harper, John H. Wright, Allyson L. Tucker, Jeffrey V. Zurawski, Laura L. Lee², Sara E. Blumer-Schuette³, and Robert M. Kelly⁴

From the Department of Chemical and Biomolecular Engineering, North Carolina State University, Raleigh, North Carolina 27695

The genome of the extremely thermophilic bacterium *Caldicellulosiruptor kronotskyensis* encodes 19 surface layer (S-layer) homology (SLH) domain-containing proteins, the most in any *Caldicellulosiruptor* species genome sequenced to date. These SLH proteins include five glycoside hydrolases (GHs) and one polysaccharide lyase, the genes for which were transcribed at high levels during growth on plant biomass. The largest GH identified so far in this genus, Calkro_0111 (2,435 amino acids), is completely unique to *C. kronotskyensis* and contains SLH domains. Calkro_0111 was produced recombinantly in *Escherichia coli* as two pieces, containing the GH16 and GH55 domains, respectively, as well as putative binding and spacer domains. These displayed endo- and exoglucanase activity on the β -1,3-1,6-glucan laminarin. A series of additional truncation mutants of Calkro_0111 revealed the essential architectural features required for catalytic function. Calkro_0402, another of the SLH domain GHs in *C. kronotskyensis*, when produced in *E. coli*, was active on a variety of xylans and β -glucans. Unlike Calkro_0111, Calkro_0402 is highly conserved in the genus *Caldicellulosiruptor* and among other biomass-degrading Firmicutes but missing from *Caldicellulosiruptor bescii*. As such, the gene encoding Calkro_0402 was inserted into the *C. bescii* genome, creating a mutant strain with its S-layer extensively decorated with Calkro_0402. This strain consequently degraded xylans more extensively than wild-type *C. bescii*. The results here provide new insights into the architecture and role of SLH domain GHs and demonstrate that hemicellulose degradation can be

enhanced through non-native SLH domain GHs engineered into the genomes of *Caldicellulosiruptor* species.

Many bacteria (1, 2) and archaea (3) produce a two-dimensional, para-crystalline array of protein that covers the outside of the cell, referred to as a surface layer (S-layer).⁵ In bacteria, the majority of S-layer proteins are non-covalently associated with the bacterial cell surface via specialized domains at their N or C terminus, typically from one of three distinct but analogous domain categories: surface layer homology (SLH) (4, 5), CWB2 (pfam04122) (6), or NCAD (previously SLAP, pfam03217) (7, 8). In archaea, S-layer proteins are most often attached to the cell membrane. S-layer proteins can be anchored to the membrane via a C-terminal transmembrane helix domain (3, 9) or covalently attached to cell membrane lipid via an archaeosortase, as shown in *Haloferax volcanii* (10, 11). In most microorganisms, the S-layer is composed entirely of one or two proteins (SLPs), which self-assemble. In addition to these SLPs, some Firmicutes produce a family of proteins that also contain SLH, CWB2, or NCAD domains and, as such, are predicted to be associated with the S-layer (12). SLPs and S-layer associated proteins can also contain domains with specialized functions allowing the S-layer to play a role in adherence and biofilm formation (13–16), biogenesis of the cell envelope (17), cell division (18), motility (19, 20), and, of interest here, plant cell wall degradation (21, 22).

Many lignocellulose-degrading bacteria utilize SLH domain-containing proteins to display plant biomass-degrading carbohydrate active enzymes (CAZymes) (23) on the cell surface. In cellulosomal bacteria, SLH domain proteins attached to the cell surface interact with the scaffoldin protein of the multienzyme cellulosome complex to anchor it to the cell surface (24–26). In many non-cellulosomal, biomass-degrading bacteria, multidomain CAZymes containing SLH proteins are implicated in lignocellulose deconstruction. About 5% of the 20,710 predicted SLH domain proteins, represented in 1889 genomes

^{*} This work was supported by the BioEnergy Science Center, a United States Department of Energy Bioenergy Research Center supported by the Office of Biological and Environmental Research in the Department of Energy Office of Science. The authors declare that they have no conflicts of interest with the contents of this article. The content is solely the responsibility of the authors and does not necessarily represent the official views of the National Institutes of Health.

[5] This article contains supplemental Table S1.

¹ Supported by United States Department of Education GAANN Fellowship P200A100004-12.

² Supported by a National Institutes of Health Biotechnology Traineeship (National Institutes of Health Grant T32 GM008776-11) and National Science Foundation graduate fellowship.

³ Present address: Dept. of Biological Sciences, Oakland University, Rochester, MI 48309.

⁴ To whom correspondence should be addressed: Dept. of Chemical and Biomolecular Engineering, North Carolina State University, EB-1, 911 Partners Way, Raleigh, NC 27695-7905. Tel.: 919-515-6396; Fax: 919-515-3465; E-mail: rmkelly@ncsu.edu.

This is an Open Access article under the CC BY license.

⁵ The abbreviations used are: S-layer, surface layer; SLH, surface layer homology (pfam00395); SLP, S-layer protein; CAZyme, carbohydrate active enzyme; GH, glycoside hydrolase; PL, polysaccharide lyase; CBM, carbohydrate binding module; FN3, fibronectin type III (pfam00041); ACL, actin cross-linking-like RICIN superfamily (CL22458); LOD, low osmolality defined; LOC, low osmolality complex; TM, truncation mutant; BisTris, 2-[bis(2-hydroxyethyl)amino]-2-(hydroxymethyl)propane-1,3-diol; DNS, 3,5-dinitrosalicylic acid.

from the Integrated Microbial Genomes database (27), contain at least one identifiable CAZyme-related component: glycoside hydrolase (GH), polysaccharide lyase (PL), carbohydrate esterase, or carbohydrate binding module (CBM).

Multidomain CAZymes containing SLH domains have been characterized from *Caldanaerobius polysaccharolyticus* (28, 29), *Bacillus* sp. (30), *Paenibacillus* sp. (31–36), *Clostridium* sp. (37–44), *Thermoanaerobacterium* sp. (45–51), and *Caldicellulosiruptor* sp. (21, 52). Across these species, the number of identifiable CAZyme domain-containing SLH proteins and total predicted SLH proteins vary significantly. Examples include *Paenibacillus* sp. strain JDR-2 (23 CAZyme domain containing of 78 total SLH domain proteins), *Clostridium thermocellum* ATCC 27405 (4 of 25), *Thermoanaerobacterium saccharolyticum* strain JW/SL-YS485 DSM 8691 (7 of 12), *Caldicellulosiruptor bescii* (1 of 12), and *Caldicellulosiruptor kronotskyensis* (6 of 19).

The genus *Caldicellulosiruptor* is composed of extremely thermophilic, Gram-positive, anaerobic bacteria that are able to attach to and degrade the variety of polysaccharides found in lignocellulosic biomass. Currently, the genomes of 12 members of the genus have been sequenced, representing species isolated from globally distributed terrestrial hot springs (53–57). *Caldicellulosiruptor* species produce many extracellular CAZymes, including some that have SLH domains (58). The enzyme inventory produced by individual species, and thus the capacity to degrade plant biomass polysaccharides, varies significantly across the genus (59, 60). *C. kronotskyensis* has the largest inventory of CAZymes of any *Caldicellulosiruptor* species, with 31 CAZymes compared with 20 CAZymes in *C. bescii*, which is to date the most studied member of the genus (61).

During growth on complex carbohydrates, *Caldicellulosiruptor* species physically associate with the substrate. This attachment is mediated in part by non-catalytic cellulose-binding proteins, called tāpirins, that were recently identified and characterized (62). In addition, proteins anchored to the cell surface within the S-layer via SLH domains are also believed to play a role in the attachment of *Caldicellulosiruptor* species to insoluble plant biomass substrates (21, 63). Two such SLH domain proteins from *C. saccharolyticus*, Csac_0678 and Csac_2722, were shown to bind to insoluble substrates and could be identified in the S-layer protein cell fraction, implying a role in cell-substrate attachment (21). However, more information is needed to understand the role of SLH domain proteins in plant biomass deconstruction, especially how their function relates to other CAZymes produced for this purpose. In this study, the localization, biochemical characteristics, and physiological role of two SLH domain enzymes from *C. kronotskyensis*, xylanase Calkro_0402 and laminarinase Calkro_0111, were examined from this perspective.

Experimental Procedures

Bacterial Strains, Plasmids, and Reagents—Cloning and expression of recombinant proteins used various *E. coli* strains: NovaBlue GigaSingles™ (EMD Millipore), Rosetta™ 2(DE3) Singles™ (EMD Millipore), NEB 10-beta electrocompetent *E. coli* (New England Biolabs), and Arctic Express (DE3)RIL *E. coli* (Agilent Technologies). Axenic strains of *C. bescii* and

C. kronotskyensis were obtained from the Leibniz Institute DSMZ-German Collection of Microorganisms and Cell Cultures. *C. bescii* strain JWC018 (64) and non-replicating vector pDCW121 (65) were obtained from J. Westpheling (University of Georgia, Athens, Georgia). Genes of interest were amplified by polymerase chain reaction (PCR) and cloned using the pET46 Ek/LIC vector kit (EMD Millipore) for protein expression. All other vectors were constructed using one-step isothermal assembly of overlapping dsDNA, as described previously (66). Plasmids were isolated using Qiaprep miniprep kits (Qiagen), and plasmid sequences were confirmed by sequencing (Genewiz). Oligonucleotide primer sequences used are listed in Table 1. Carbohydrates and biomasses used included the following: laminarin from *Laminaria digitata* (Sigma L9634), xylan from birchwood (Sigma X0502), xylan from oat spelts (Sigma X0627), and dilute acid-pretreated *Populus trichocarpa* × *Populus deltoides* (National Renewable Energy Laboratory, Golden, CO).

Growth Media and Culture Conditions—All *E. coli* cultures were maintained in Luria-Bertani (LB) medium (5 g/liter yeast extract, 10 g/liter tryptone, 10 g/liter NaCl) or LB medium with 1.5% (w/v) agar plates supplemented with 50 µg/ml carbenicillin (Corning Cellgro), 34 µg/ml chloramphenicol (Sigma), 20 µg/ml gentamycin (Chem-Impex International Inc.), 50 µg/ml streptomycin (Sigma), and/or 50 µg/ml apramycin (Fisher), as appropriate. Protein expression was performed in either Terrific Broth medium (containing 12 g/liter tryptone, 24 g/liter yeast extract, 4 ml/liter glycerol, 2.31 g/liter KH₂PO₄, and 12.54 g/liter K₂HPO₄) or ZYM-5052 medium (67) modified to contain 0.625% glycerol, 0.0625% glucose, and 0.25% lactose.

Caldicellulosiruptor strains were grown anaerobically at 70 °C in modified DSM640 medium (DSMZ), containing 0.9 g/liter NH₄Cl, 0.9 g/liter NaCl, 0.4 g/liter MgCl₂·6H₂O, 0.75 g/liter KH₂PO₄, 1.5 g/liter K₂HPO₄, 1 g/liter yeast extract, 1 ml/liter trace element solution SL-10, 5 g/liter cellobiose, 0.5 mg/liter resazurin, and 0.75 g/liter L-cysteine-HCl×H₂O. *Caldicellulosiruptor* genomic DNA for cloning and vector construction was extracted, as described previously (68). For genetic manipulations of *C. bescii*, strains were grown anaerobically at 70 °C in low osmolality defined (LOD) or low osmolality complex (LOC) medium (69). *C. bescii* was plated embedded in LOD medium with 1.5% agar and grown at 70 °C in anaerobic tanks with N₂ head space. For solubilization experiments and immunofluorescence microscopy, *Caldicellulosiruptor* strains were grown on a modified defined version of DSMZ671 medium (671d medium), described previously (70), with 5 g/liter of the specific biomass substrate as the carbon source. For growth of all uracil auxotroph mutants, growth medium was supplemented with 40 mM uracil.

Expression of Recombinant Proteins in *E. coli*—All Calkro_0111 truncation mutants (TMs) and Calkro_0402 TM1 were cloned into the pET46 Ek/LIC vector maintained in NovaBlue *E. coli*. Sequence confirmed plasmids were transformed into Rosetta 2(DE3) *E. coli* for protein expression. Proteins were expressed in modified ZYM-5052 autoinduction medium at 37 °C 250 rpm. Cells were harvested 18–24 h after induction by centrifugation at 6,000 × g for 10 min. For the expression of Calkro_0402, the gene was cloned into the pET46 Ek/LIC vec-

TABLE 1

Primers used in this study

Underlined portions are vector-specific or overlap regions for isothermal assembly.

Primer	Sequence	Use
Calkro_0111 TM1 F	<u>GACGACGACAAGATAAAATAAGCAGGCACA</u>	pET46 cloning
Calkro_0111 TM1/TM3 R	<u>GAGGAGAAGCCCGGTTAATCTGACATATCTGATTC</u>	pET46 cloning
Calkro_0111 TM2 F	<u>GACGACGACAAGATGGTTGAAAAAGGATATTTGATTGG</u>	pET46 cloning
Calkro_0111 TM2 R	<u>GAGGAGAAGCCCGGTTAACTTGGAGGGTTAGGATAAA</u>	pET46 cloning
Calkro_0111 TM3/TM4 F	<u>GACGACGACAAGATGGGTGAATGGAACTTGT</u>	pET46 cloning
Calkro_0111 TM4 R	<u>GAGGAGAAGCCCGGTTACGGTGTAGAATAGATGATGAA</u>	pET46 cloning
Calkro_0111 TM5 F	<u>GACGACGACAAGATTCCTTCCGTGGGTGAATGGAACTTGTATGG</u>	pET46 cloning
Calkro_0111 TM5 R	<u>GAGGAGAAGCCCGGTTAACCTTCTCTTTGGTATAC</u>	pET46 cloning
Calkro_0111 TM6 F	<u>GACGACGACAAGATGATTTTAGGATTAGGT</u>	pET46 cloning
Calkro_0111 TM6 R	<u>GAGGAGAAGCCCGGTTACAATTTCTTTTCTAAAGAT</u>	pET46 cloning
Calkro_0111 TM7 F	<u>GACGACGACAAGATCTCTGGAGGCAGGTCTTA</u>	pET46 cloning
Calkro_0111 TM7 R	<u>GAGGAGAAGCCCGGTTAGGTTTCTCCATTTTCATTG</u>	pET46 cloning
Calkro_0111 TM8 F	<u>GACGACGACAAGATGACAGATACAGGTTTGAG</u>	pET46 cloning
Calkro_0111 TM8 R	<u>GAGGAGAAGCCCGGTTACTTGCTCCCATACAC</u>	pET46 cloning
Calkro_0111 TM9 F	<u>GACGACGACAAGATGTCTAGAGCCTATATCT</u>	pET46 cloning
Calkro_0111 TM9 R	<u>GAGGAGAAGCCCGGTTACTTGCTCCCATACACTTCA</u>	pET46 cloning
Calkro_0111 TM10 F	<u>GACGACGACAAGATGTTTGGTCCAAATGTCTA</u>	pET46 cloning
Calkro_0111 TM10 R	<u>GAGGAGAAGCCCGGTTAGTTGCAATATTCTGTTAC</u>	pET46 cloning
Calkro_0402 F	<u>GACGACGACAAGATTCAAAGCAGCCAACTAA</u>	pET46 cloning
Calkro_0402 R	<u>GAGGAGAAGCCCGGTTACTTTTGAGATTGTTAAGTGCTCTG</u>	pET46 cloning
Calkro_0402 TM1 F	<u>GACGACGACAAGATGTCTAGATAGCATAAAG</u>	pET46 cloning
Calkro_0402 TM1 R	<u>GAGGAGAAGCCCGGTTATTGAGCATTTCTTGTAACTG</u>	pET46 cloning
ΔAthe_2438 5' F	<u>GAGTGTAGGCTGGTGTACCCATACACCAAAATGATATAATCTCC</u>	pJMC009
ΔAthe_2438 5' R	<u>TAAATCCTGTTTATCATGTTGGAAGGCCAAATTG</u>	pJMC009
Cbscii Pslp (Athe_2303 promoter) F	<u>AACATGATAAACAGGATTTAAAGAGGGCTATG</u>	pJMC009
Cbscii Pslp (Athe_2303 promoter) R	<u>GCTTTTTCATAACTACTACCAAACTC</u>	pJMC009
Calkro_0402 + Calkro Terminator F	<u>GTGAGTAGTTATGAAAAAGCGACTTATAGC</u>	pJMC009
Calkro_0402 + Calkro Terminator R	<u>CTACCTAATCGGAAGACTAAAGATTTTCTCC</u>	pJMC009
ΔAthe_2438 3' F	<u>TTAGTCTTCCGATTAGGTAGGTGGTTTTAAC</u>	pJMC009
ΔAthe_2438 3' R	<u>CAGTGAAGCGTCAGAGAATTCGGATTATCGCTGAGTTG</u>	pJMC009
pDCW121 backbone F	<u>GAATCTCTGACGCTCAG</u>	pJMC009
pDCW121 backbone R	<u>GGTACCACCAGCCTAACCTC</u>	pJMC009
ΔAthe_2438 locus F	<u>GGCAACCTTCAGTAGGCTGC</u>	PCR
ΔAthe_2438 locus R	<u>CATTGATATCAGAATGTTCTCGTTGATT</u>	PCR

tor without the predicted signal peptide, as determined by the SignalP 4.1 server (71), and maintained in NEB 10-beta *E. coli*. The sequence-confirmed plasmid was transformed into Arctic Express (DE3)RIL *E. coli* for protein expression. Expression was performed in Terrific Broth medium by growing cells at 30 °C and 250 rpm until A_{600} reached 1.0 followed by induction at 13 °C with 1 mM isopropyl- β -D-thiogalactopyranoside. Cells were harvested 16–20 h later by centrifugation at $6,000 \times g$ for 10 min. All cell pellets were frozen at -20 °C prior to purification.

Purification of Recombinant Protein and Truncation Mutants—Cell pellets were resuspended in 5 ml of 20 mM sodium phosphate, pH 7.4, 0.5 M NaCl, 20 mM imidazole, 0.1% (v/v) Nonidet P-40, and 1 mg/ml lysozyme per g of wet cell pellet. Cells were lysed in a French press at 16,000 p.s.i. Cell lysates were heat-treated at 65 °C for 20 min (except for the full-length Calkro_0402 protein product which was not heat-treated) to remove heat-labile proteins from *E. coli*. The cell lysate was then centrifuged at $25,000 \times g$ for 20–60 min, and the supernatant was passed through a 0.22- μ m filter to prepare cell-free cell extract. Proteins were purified using 1- or 5-ml HisTrap HP nickel-Sepharose (GE Healthcare) immobilized metal affinity chromatography columns, operated according to the manufacturer's instructions. For full-length Calkro_0402 and Calkro_0111 TM8, size exclusion chromatography was used after immobilized metal affinity chromatography on a HiLoad 26/600 Superdex 200 pg column (GE Healthcare) in 50 mM sodium phosphate, 150 mM NaCl, pH 7.2, buffer. All chromatography steps were performed on a Biologic DuoFlow

FPLC (Bio-Rad). Purity of the recombinant proteins was evaluated by SDS-PAGE using NuPAGE Novex 4–12% BisTris protein gels (Life Technologies, Inc.) or 4–15% Mini-PROTEAN TGX gels (Bio-Rad) with a Benchmark protein ladder (Life Technologies) and staining by GelCode Blue Safe Protein Stain (Thermo Scientific). The concentration of purified proteins was determined using the bicinchoninic acid assay (Pierce).

Optimal pH and Temperature Determination—The pH optimum for each recombinant enzyme was determined at 70 °C in buffers at pH 2.5–10 (50 mM citrate buffer, pH 2.5 and 3.5; 50 mM sodium acetate buffer, pH 4.5, 5, 5.5, and 6; 50 mM sodium phosphate, pH 6.5, 7, and 8; 50 mM sodium bicarbonate, pH 9.2 and 10). The temperature optimum was determined at the optimal pH between 30 and 100 °C. Enzyme reactions and no enzyme/substrate controls were prepared in triplicate with 100 μ l of 1% substrate and incubated in PCR multiwell plates in a thermocycler (Eppendorf). Activity was assessed by measuring reducing sugar released using a 3,5-dinitrosalicylic acid (DNS) assay (modified from Refs. 72 and 73 and adapted to a 96-well microplate format (74, 75)). The DNS reagent used contained 1.6% (w/v) sodium hydroxide, 30% (w/v) sodium potassium tartrate, and 0.1% (w/v) 3,5-dinitrosalicylic acid. Briefly, 30 μ l of sample was mixed with 60 μ l of DNS reagent and incubated in a 96-well PCR plate in a thermocycler (Eppendorf) using the following program: 95 °C for 5 min, 48 °C for 1 min, hold at 20 °C. Then the DNS reaction was diluted with distilled water, and absorbance was measured at 540 nm. Glucose or xylose was used as a standard for glucooligosaccharide or xylooligosaccharide release.

Analysis of Oligosaccharide Products from Enzymatic Hydrolysis—To analyze oligosaccharides released by the various enzymes, enzyme was added to 500 μ l of 1% substrate in buffer at the enzyme's optimum pH and incubated between 0 and 240 min at 70 °C at 800 rpm in a mixing thermocycler (Eppendorf). Reactions without substrate and/or enzyme were also assessed. After incubation, tubes were spun at $16,000 \times g$ for 5 min at 4 °C, and the supernatant was applied to 0.5 ml of 10,000 molecular weight cut-off protein concentrators (Pierce). The protein concentrator eluent was diluted 10-fold with distilled water and analyzed by high performance liquid chromatography (HPLC) (Alliance e2695 separations module, Waters) with refractive index (model 2414, Waters) and photodiode array (model 2998, Waters) detectors. Columns were either the KS-801 (xylooligosaccharides) or KS-802 (glucooligosaccharides) (Shodex) operated with water as the mobile phase (0.6 ml/min and 80 °C). Laminarioligosaccharides (L2–L6) (Seikagaku Corp.), individual xylooligosaccharides (X2–X6) (Megazyme), glucose (Sigma), and xylose (Acros Organics) were used as standards.

Confocal and Epifluorescence Microscopy—All centrifugation steps for the preparation of labeled cells were carried out at $6,000 \times g$ for 10 min. Cells harvested from a 50-ml culture in 671d medium were washed one time with sterile $1\times$ phosphate-buffered saline (PBS), and cells were fixed in $1\times$ PBS containing 4% formaldehyde (methanol-free; Fisher) for 30 min at room temperature with gentle shaking, followed by washing three times with 50 ml of PBS. Cells were resuspended in 3 ml of antibody-blocking solution containing 5% (v/v) normal goat serum (Immunoreagents), 1% (w/v) bovine serum albumin (protease- and nuclease-free; Fisher), and 0.05% (v/v) Tween 20 (Fisher) in PBS and incubated on a Boeckle rocker for 60 min at room temperature. After this blocking step, cells were harvested by centrifugation and resuspended in antibody blocking solution containing 100 μ g/ml primary antibody. Polyclonal antibodies were raised against Calkro_0111 TM7 or Calkro_0402 TM1 in chickens and supplied as total IgY with preimmune total IgY controls by GeneTel Laboratories (Madison, WI). Cells were incubated with the primary antibody for 18 h at 4 °C on a Boeckle rocker. After this incubation, cells were washed three times with 1 ml of PBS containing 1% (w/v) bovine serum albumin and 0.05% (v/v) Tween 20 and resuspended in antibody blocking solution containing a 1:400 dilution of goat anti-chicken DyLight488-conjugated secondary antibody (Immunoreagents) and incubated on a Boeckle rocker for 60 min at room temperature. Cells were harvested and washed three times with PBS, resuspended in 100 μ l of 3.6 μ M DAPI in PBS, and incubated at 4 °C for 18 h. Following this incubation, cells were washed three times, resuspended with PBS, and vacuum-filtered onto 0.22- μ m polycarbonate hydrophilic isopore membrane filters (EDM Millipore) and mounted in 15 μ l of SlowFade Diamond anti-fade mountant (Life Technologies). For Calkro_0111 and Calkro_0402 localization in *C. kronotskyensis*, slides were imaged on a Zeiss LSM 710 confocal work station using a $\times 63$ oil immersion plan-apochromat (numerical aperture 1.4) objective (North Carolina State University Cellular and Molecular Imaging Facility, Raleigh, NC). Image processing was performed using Zeiss Zen Blue software.

Epifluorescence imaging and cell counting were performed using a Nikon eclipse 50i microscope with a Plan Fluor $\times 100$ (numerical aperture 1.3) oil emersion objective and Nikon DS-Fi1 camera. For routine cell counting, cells were stained with acridine orange, as described previously (76). For immunofluorescence images of *C. bescii* genetic mutant strains, cells were labeled and slides were prepared as described above for confocal imaging. Images were captured as a z-stack of images through the sample with 0.33- μ m steps controlled by the ES10ZE Focus controller (Prior Scientific) and processed into a single focused image using the Nikon Elements software extended depth of field processing methods. Transmission electron microscopy was performed at the Laboratory for Advanced Electron and Light Optical Methods (College of Veterinary Science, North Carolina State University).

Genetic Manipulation of *C. bescii*—To prepare competent cells, a 500-ml culture of *C. bescii* strain JWC018 was grown to an optical density at 680 nm of 0.06–0.07 in LOD medium supplemented with $1\times$ 19-amino acid solution (77). The culture was cooled to room temperature, and cells were harvested by centrifugation. All centrifugation steps were carried out at $6,000 \times g$ for 10 min. The cell pellet was washed three times with 10% sucrose and resuspended with 10% sucrose to a total volume of 100–120 μ l. Fifty μ l of competent cells were mixed with 1 μ g of pJMC009 plasmid DNA at room temperature and electroporated using 1-mm gap cuvettes (USA Scientific) and a Gene Pulser II system with a Pulse Controller PLUS module (Bio-Rad) operated at 2.25 kV, 600 ohms, and 25 microfarads. Immediately following electroporation, cells were transferred to 10 ml of prewarmed LOC medium and incubated at 70 °C for 1 h. After this incubation, the culture was cooled to room temperature, and cells were harvested by centrifugation, transferred to 100 ml of prewarmed LOD medium lacking uracil, and incubated at 70 °C for 2–4 days to select for first crossover transformants. This culture was passaged and then plated on LOD medium lacking uracil to select individual colonies. Integration of the pJMC009 vector was confirmed by PCR, and a successful first crossover mutant strain was plated on LOD medium supplemented with 40 mM uracil and 4 mM 5-fluoroorotic acid to select for second crossover mutants. Isolated colonies were screened by PCR, and successful second crossovers were identified. A successful second crossover was plated on LOD medium supplemented with uracil, and individual colonies were isolated. This plating and isolation of colonies was repeated two times to obtain the final strain and ensure its purity. All PCR screening steps were performed using genomic DNA isolated using the ZymoBeadTM genomic DNA kit (Zymo Research).

Hydrolysis of Hemicellulose Substrates—Washed biomass substrates (oat spelt xylan, birchwood xylan) were prepared by washing 1 g of substrate/100 ml of distilled water overnight at 70 °C to remove soluble sugars, centrifuging at $6,000 \times g$ for 10 min, and drying at 70 °C. *Caldicellulosiruptor* strains were passaged on modified 671d medium with respective biomass substrates 3–4 times. Solubilization cultures were prepared in triplicate as 50-ml 671d medium cultures with 5 g/liter substrate, inoculated to 1×10^6 cells/ml, and grown at 70 °C for 45.5 h. Residual substrate was harvested by centrifugation at $6,000 \times g$

C. kronotskyensis SLH Glycoside Hydrolases

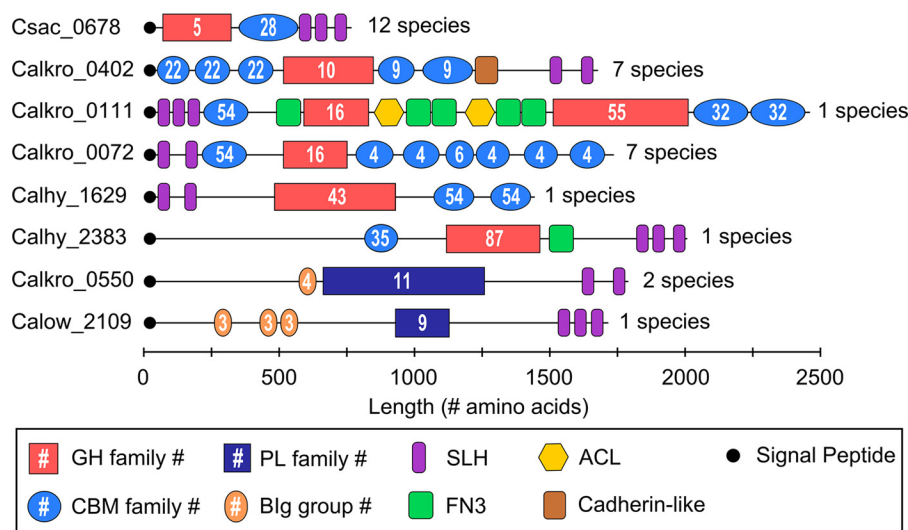


FIGURE 1. **Catalytic CAZyme SLH domain proteins from the genus *Caldicellulosiruptor*.** Domain arrangement of these multidomain proteins is drawn to scale based on a prediction from the NCBI conserved domain database (93) and Pfam protein families database (94). Representative genes for each group containing more than one member are shown on the left. The number of *Caldicellulosiruptor* species genomes from the 12 completely sequenced to date that contain a member from each group is shown to the right. *Blg*, bacterial immunoglobulin-like (CL0159); *Cadherin-like* (pfam12733).

for 10 min and drying at 70 °C until constant mass. The extent of solubilization was determined from the difference in mass between the biomass used to prepare each culture and the residual remaining after harvest. For time course analysis of oat spelt xylan solubilization, cultures were prepared as above except that cultures were sampled by removing 2 ml of culture and centrifuging the samples at $6,000 \times g$ for 10 min. The supernatant was stored at -20°C prior to HPLC analysis.

Analysis of Solubilization in Culture Supernatants—Supernatant samples were analyzed for xylose content, as described previously (70). Briefly, the samples were brought to 4% (w/w) sulfuric acid and autoclaved for 1 h on the liquid cycle. Samples were cooled to room temperature and spun at $18,000 \times g$ for 5 min, and supernatant was analyzed by HPLC as described above except using an Aminex-87H (300×7.8 mm; Bio-Rad) column with a mobile phase of 5 mM sulfuric acid at 0.6 ml/min and 60 °C.

C. kronotskyensis and C. bescii RNA Microarray—Transcriptomic data, which were acquired previously (70) and deposited in the NCBI Gene Expression Omnibus database (accession number GSE68810), were reanalyzed with respect to the SLH domain-containing proteins from *C. bescii* and *C. kronotskyensis*.

Results

SLH Domain Proteins in *Caldicellulosiruptor* Species—The genomes of the 12 sequenced *Caldicellulosiruptor* species collectively encode 34 different groups of SLH domain-containing proteins (supplemental Table S1). About half of the SLH domain-containing protein groups in these genomes have no additional identifiable domains other than SLH domains, highlighting the limited understanding of this group of proteins. *Caldicellulosiruptor* species produce between 10 (*C. saccharolyticus* and *Caldicellulosiruptor acetigenus*) and 19 (*C. kronotskyensis*) SLH domain proteins.

Eight of the 34 SLH domain-containing protein groups contain identifiable catalytic GH or PL CAZyme domains (Fig. 1).

Csac_0678 (GH5), which has been characterized previously (21), has homologs in all 12 sequenced *Caldicellulosiruptor* species. Three of the 12 *Caldicellulosiruptor* species (*Caldicellulosiruptor owensensis*, *Caldicellulosiruptor obsidiansis*, and *Caldicellulosiruptor* sp. strain Rt8.B8) only produce a truncated homolog of Csac_0678 (see supplemental Table S1). Homologs of Calkro_0402 (GH10) are found in seven sequenced *Caldicellulosiruptor* species, with 65–83% amino acid sequence identity. One ortholog of Calkro_0402 (76% identity) has been characterized from *Caldicellulosiruptor* sp. Rt69.B1 (52), which does not have a fully sequenced genome. Calkro_0402 and its *Caldicellulosiruptor* sp. homologs belong to a larger group of GH10 enzymes with similar domain architecture, both with and without C-terminal SLH domains, that have been characterized from several xylan-degrading microbes (28, 31, 33, 34, 36, 37, 39–46, 48–51, 78).

The other six groups of catalytic SLH domain proteins (Fig. 1) have not been characterized from *Caldicellulosiruptor* species. Calkro_0111 (GH16/GH55) is the largest of all of these at 2,435 amino acids and is also the largest CAZyme of any kind identified so far in the genus *Caldicellulosiruptor*. Calkro_0121 is a second truncated paralog of Calkro_0111, which has 60% amino acid identity to Calkro_0111 and identical domain architecture but is lacking the final CBM32 domain. The arrangement of the domains in Calkro_0111 and Calkro_0121 is entirely unique to *C. kronotskyensis*, and no homologs of the full protein (Calkro_0111) can be identified in any other sequenced microorganism. Calkro_0072 (GH16) has homologs in seven *Caldicellulosiruptor* species and is very similar to the β -1,3-glucanase Lic16A characterized from *C. thermocellum* (38). *C. hydrothermalis* produces two catalytic SLH domain proteins that are unique to this species, putative xylanase Calhy_1629 (GH43) and putative α -glucanase Calhy_2383 (GH87). Calkro_0550 (PL11) from *C. kronotskyensis* has one additional homolog in *C. owensensis* and is a putative rhamnogalacturonan lyase. *C. owensensis* also produces one other putative pec-

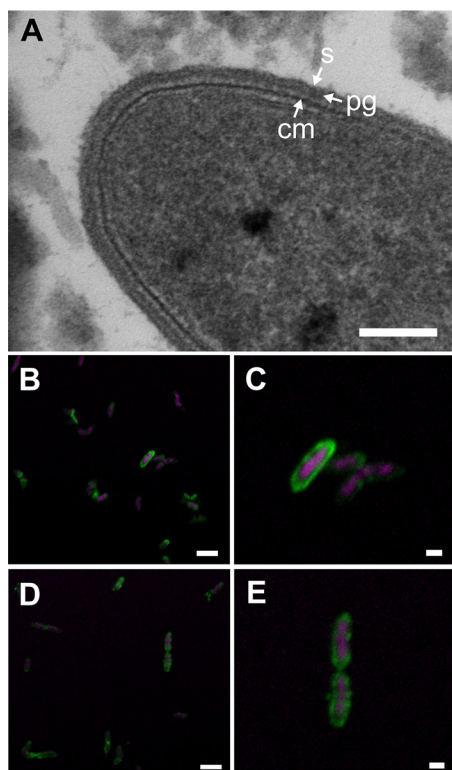


FIGURE 2. Transmission electron microscopy and immunofluorescence microscopy of *C. kronotskyensis*. A, transmission electron microscopy of *C. kronotskyensis* grown on dilute acid-pretreated *P. trichocarpa* × *P. deltoides* showing the cytoplasmic membrane (cm), peptidoglycan (pg), and S-layer (s). B and C, confocal microscopy of *C. kronotskyensis* grown on laminarin labeled with total IgY antibodies raised against Calkro_0111 TM7. C and D, confocal microscopy of *C. kronotskyensis* grown on xylooligosaccharides labeled with total IgY antibodies raised against Calkro_0402 TM1. The cell counterstain (DAPI) is shown in magenta, and secondary antibody labeling (DyLight488 goat anti-chicken) is shown in green. Scale bars, 100 nm (A), 4 μ m (B), 1 μ m (C), 4 μ m (D), and 1 μ m (E).

tate lyase SLH domain protein, Calow_2109 (PL9), which is unique to this species.

These catalytic SLH domain proteins encompass a range of enzymatic activities localized in the S-layer, presumably used to break down plant polysaccharide components that are in proximity of the cell surface. *C. kronotskyensis* produces six CAZyme SLH domain proteins, the most of any species; *C. bescii* only produces one, a homolog of Csac_0678, which is conserved in all *Caldicellulosiruptor* species. These SLH-localized CAZymes accompany a host of other CAZyme domains found in extracellular free enzymes produced by *Caldicellulosiruptor* sp. for plant biomass degradation (58).

C. kronotskyensis Produces an S-layer and SLH Enzymes Calkro_0111 and Calkro_0402 Are Localized on the *C. kronotskyensis* Cell Surface—Transmission electron microscopy of *C. kronotskyensis* growing on dilute acid-treated poplar (*P. trichocarpa* × *P. deltoides*) shows the cell membrane, peptidoglycan layer, and S-layer of *C. kronotskyensis* cells (Fig. 2A), with the cells appearing to attach to granules of the substrate mediated by appendages at the cell surface. To determine the localization of the SLH CAZymes Calkro_0402 and Calkro_0111, polyclonal antibodies were raised against portions of these proteins and used for immunofluorescence microscopy in *C. kronotskyensis*. Fig. 2, panels B and C and pan-

els D and E, shows confocal microscopy of *C. kronotskyensis* labeled with anti-Calkro_0111 and anti-Calkro_0402 antibodies, respectively. Controls labeled with preimmune total IgY antibodies show minimal labeling (data not shown). In each case, these enzymes are localized on the cell surface within the S-layer, as would be predicted by the presence of SLH domains. Because of the high similarity between Calkro_0111 and Calkro_0121, the antibodies are probably labeling both of these proteins in Fig. 2 (B and C).

Laminarinase Calkro_0111 Displays Endo- and Exoglucanase Activity in Separate Catalytic Domains—Calkro_0111 contains 15 predicted domains, including the two catalytic units: GH16 and GH55 (Fig. 3A). Because the full enzyme could not be produced recombinantly in *E. coli*, the enzyme was split into several TMs for characterization. Two of these TMs were used to characterize the enzymatic activity: TM1, containing the GH16 domain and covering the first half of Calkro_0111, and TM8, containing the GH55 domain and covering the second half of Calkro_0111. For both TM1 and TM8, the optimal pH was 5, whereas the optimal temperature was 75 °C (Fig. 3B). Analysis of the oligosaccharides released from laminarin by these two halves of Calkro_0111 showed that the GH55 domain of TM8 generates primarily glucose and a small amount of laminaribiose from laminarin, whereas the GH16 domain of TM1 released laminooligosaccharides of size L3 (laminaritriose) and greater, which slowly accumulated with time (Fig. 3C). Taken together, these findings suggest that the GH16 domain is an endoglucanase, whereas the GH55 domain is an exoglucanase. Considering the full-length enzyme, coordination between the GH16 and GH55 domains is expected, such that the GH16 cuts new chain ends for the GH55 to digest, thereby liberating glucose. This synergism is not uncommon in freely secreted *Caldicellulosiruptor* enzymes with two catalytic domains (76, 79, 80), but synergism had yet to be demonstrated in any CAZyme SLH domain protein. This is primarily due to the fact that very few SLH domain proteins have two catalytic CAZyme domains, further highlighting the uniqueness of Calkro_0111.

To further explore the domain arrangement and the contribution of the non-catalytic domains to activity, a range of TMs (Fig. 3A) were produced in *E. coli* and analyzed. Activity of these TMs at 70 °C on laminarin was evaluated at pH 5, the enzyme optimum pH, and pH 7, the growth optimum pH for *Caldicellulosiruptor* (Fig. 3D). TM3 and TM4 had the highest activity at both pH levels tested, whereas TM1 was slightly less active. TM2, which is truncated between the GH16 and the first actin cross-linking-like (ACL) domain, was significantly less active. TM5, which contains the GH16 domain alone, and TM6 and TM7, which contain the ACL and fibronectin type-III (FN3) domains and not the GH16, all displayed little to no activity (Fig. 3D). TM4, which contains the GH16 and first ACL domain, represents the smallest portion of the GH16 side of the enzyme that remains fully active under these conditions. This suggests that the ACL domain plays an important role in GH16 function. The ACL domain could stabilize the GH16 domain, a role that has been shown before for accessory domains in other GH multidomain enzymes. For example, two FN3 domains (also previously called X1 modules) of CbhA (*C. thermocellum*

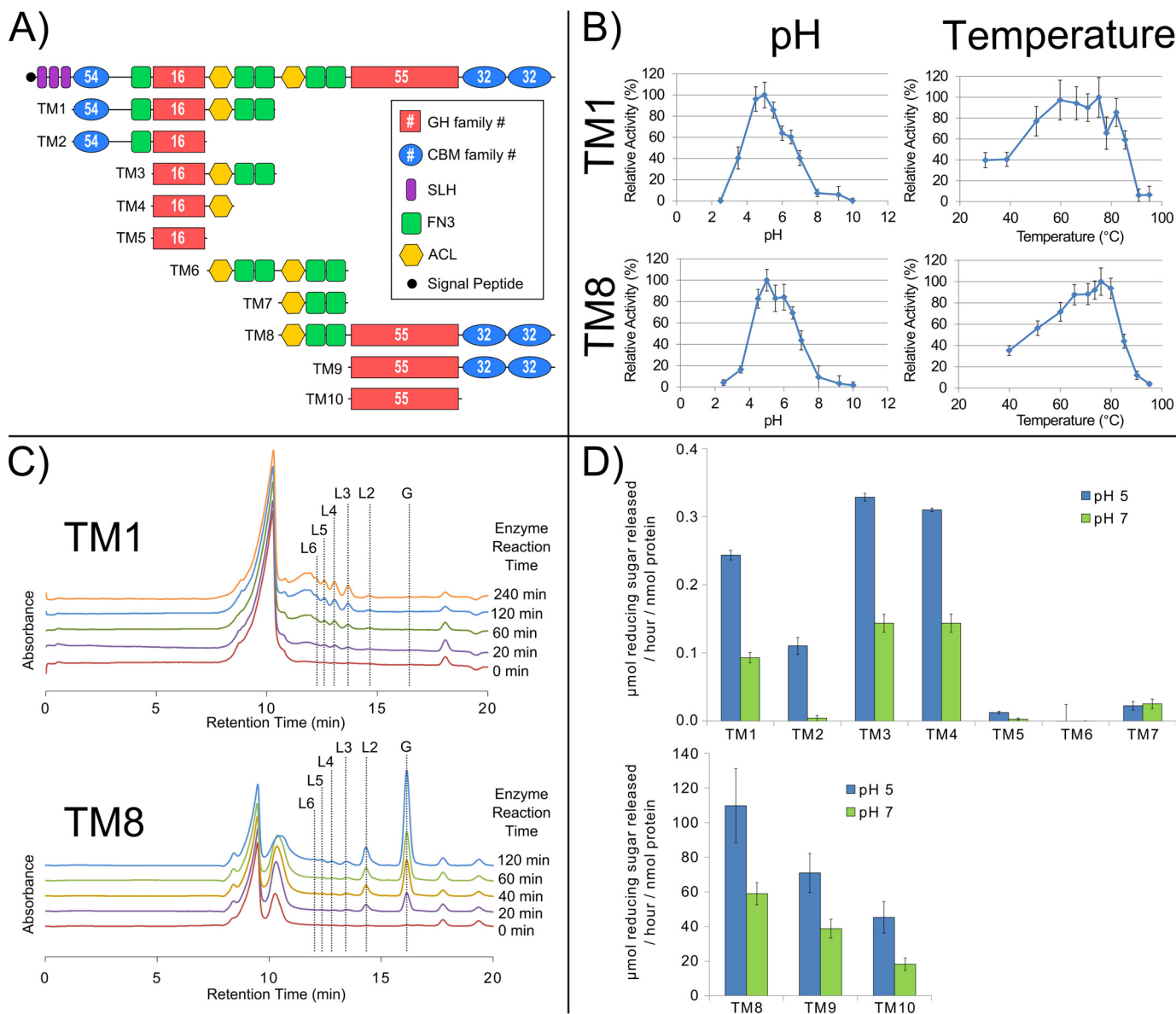


FIGURE 3. Biochemical characterization of Calkro_0111. A, domain organization for full-length Calkro_0111 and TMs produced in *E. coli* used for characterization. B, optimum pH at 70 °C and optimum temperature at the optimum pH were determined for Calkro_0111 TM1 (0.9 mg/ml, incubated for 5 h) and TM8 (0.005 mg/ml, incubated for 30 min) on the substrate laminarin. Error bars, S.D. ($n = 3$). C, oligosaccharides released from laminarin by TM1 and TM8. HPLC chromatograms for each enzyme reaction time are aligned with respect to retention time and graphed together. The location of the peaks for standards glucose (G), laminaribiose (L2), laminaritriose (L3), laminaritetraose (L4), laminaripentaose (L5), and laminarihexaose (L6) are shown. D, truncation mutant activity as measured by the DNS reducing sugar assay. TM1 to TM5 and TM7 (4.2 μM) were incubated for 5 h, TM6 (12.3 μM) was incubated for 10 h, and TM8 to TM10 (0.2 μM) were incubated for 30 min with 1% (w/v) laminarin at 70 °C and pH 5 or 7. Activity is calculated in μmol of reducing sugar released/h/nmol of protein to compare activity for the proteins of different mass. Error bars, S.D. ($n = 3$).

cellobiohydrolase A) increased the thermostability of the adjacent GH9 domain (81). For the Calkro_0111 GH55 domain, removal of the ACL and FN3 domains from TM8 to TM9 and then removal of the two CBM32 domains from TM9 to TM10 resulted in successive reductions in activity (Fig. 3D). This suggests that both the ACL-FN3-FN3 grouping and two CBM32 domains play an important role in the activity of the Calkro_0111 GH55.

Biochemical Characterization of Calkro_0402 and Relatedness to Other CBM22/GH10/CBM9 Enzymes—Calkro_0402 belongs to a large group of homologous CBM22-, GH10-, and CBM9-containing proteins, from a variety of bacteria, primarily Firmicutes. An unrooted neighbor-joining phylogenetic tree con-

structed from the full amino acid sequences of top blastp hits to Calkro_0402 and similar xylanases that have been previously characterized shows the relatedness of xylanase enzymes from this group (Fig. 4A).

Calkro_0402 contains three CBM22, one catalytic GH10, two CBM9 domains, and one cadherin-like domain, in addition to C-terminal SLH domain repeats (Fig. 4B). Full-length Calkro_0402 was produced recombinantly in *E. coli* (Fig. 4C), and the optimal pH and temperature for activity on birchwood xylan were found to be pH 5.5 and 80 °C, respectively (Fig. 4D). Calkro_0402 releases primarily xylotri- and xylobiose from birchwood xylan but also a small amount of xylose (Fig. 4E). This type of activity is consistent with other xylanase homologs

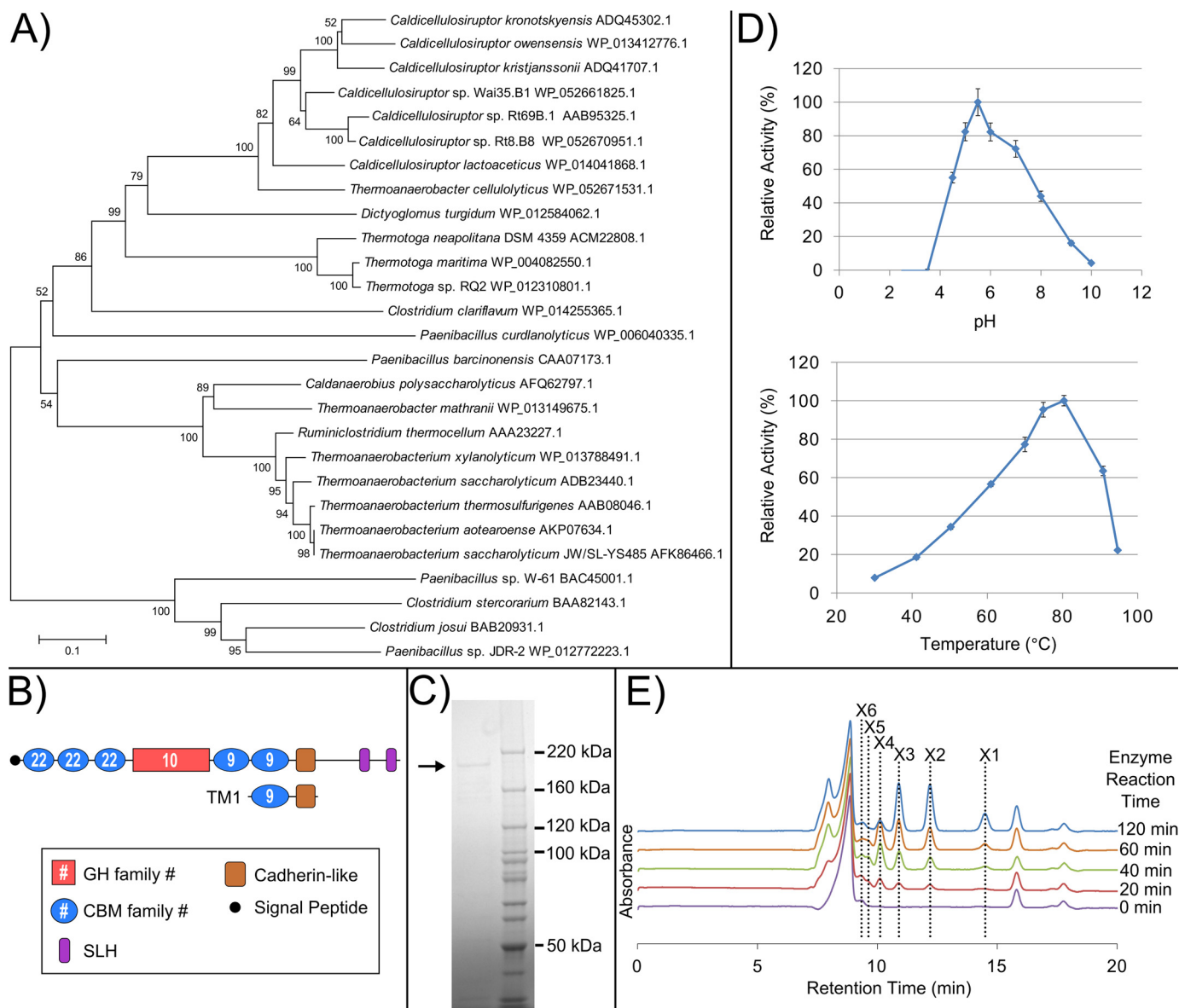


FIGURE 4. Biochemical characterization of Calkro_0402. A, MEGA version 6 (95) was used to align, using MUSCLE (96), full protein amino acid sequences and construct an unrooted neighbor-joining phylogenetic tree of close blastp homologs to Calkro_0402 and previously characterized CBM22/GH10/CBM9-containing enzymes. Species and protein accession number are shown for each enzyme branch. B, domain organization for Calkro_0402 and TM1, which was used as the antigen for antibody production. Cadherin-like (pfam12733). C, purified full-length Calkro_0402 (~180 kDa) produced in *E. coli* and purified by immobilized metal affinity and size exclusion chromatography. D, optimum pH at 70 °C and the optimum temperature at this optimum pH were determined for recombinant Calkro_0402 (0.02 mg/ml incubated 30 min). Error bars, S.D. ($n = 3$). E, oligosaccharides released from birchwood xylan by Calkro_0402. HPLC chromatograms for each enzyme reaction time are aligned with respect to retention time and graphed together. The location of the peaks for the standards xylose (X1), xylobiose (X2), xylotriose (X3), xylotetraose (X4), xylopentose (X5), and xylohexaose (X6) are shown.

that have been characterized previously (28, 31). Activity of Calkro_0402 was also detected on oat spelt xylan, wheat arabinoxylan, pachyman 1,3- β -glucan, barley β -glucan, and lichenan in addition to birchwood xylan, all at pH 5.5 and 70 °C (data not shown).

Transcriptomic Analysis of SLH Domain Proteins in *C. bescii* and *C. kronotskyensis*—Transcriptomic analysis was performed on *C. kronotskyensis* and *C. bescii*, the *Caldicellulosiruptor* species with the most and least catalytic CAZyme SLH domain proteins, respectively, when these species were grown on Avicel (crystalline cellulose) and, the more heterogeneous substrate, switchgrass. All CAZyme SLH domain proteins from both species, except Calkro_0111 and Calkro_0121, were up-

regulated on switchgrass. This transcriptional response to switchgrass suggests that these genes respond to components of switchgrass, like hemicellulose polysaccharides, not found in crystalline cellulose Avicel. The transcriptional level of these genes on switchgrass is similar to the free enzymes in the glucan degradation locus, known to be a genomic feature of cellulolytic *Caldicellulosiruptor* sp. (59, 61, 70). Calkro_0333 and Athe_2303 are very highly transcribed under both conditions. These proteins are homologs of Csac_2451, which was previously identified as the main SLP (59, 60). A number of other non-catalytic SLH domain proteins are transcribed at moderate to high levels, but because domains other than SLH domains are not predicted, the role of these proteins is unknown.

C. kronotskyensis SLH Glycoside Hydrolases

Surface Layer Homology (SLH) Domain Containing Proteins					C. bescii			C. kronotskyensis		
	Athe_	Calkro_	# AA	Domains	Avicel LSM	SWG LSM	Avicel - SWG	Avicel LSM	SWG LSM	Avicel - SWG
GH	Athe_0594	Calkro_2036	755-756	GH5-CBM28-SLH-SLH-SLH	1.2	1.9	-0.7	2.5	3.5	-1.0
		Calkro_0072	1732	SLH-SLH-SLH-CBM54-GH16-CBM4-CBM4-CBM6-CBM4-CBM4				-1.8	0.0	-1.8
		Calkro_0402	1672-1675	CBM22-CBM22-CBM22-GH10-CBM9-CBM9-SLH-SLH				0.5	3.0	-2.4
		Calkro_0111	2435	SLH-SLH-SLH-CBM54-FN3-GH16-ACL-FN3-FN3-				-1.4	-1.3	0.0
		Calkro_0121*	2229	ACL-FN3-FN3-GH55-CBM32*-CBM32				-1.9	-1.7	-0.2
PL		Calkro_0550	1789-1790	Big4-PL11-SLH-SLH				-2.1	0.3	-2.5
Other	Athe_0438	Calkro_2198	1156-1157	SLH-SLH-Big5	0.0	-0.2	0.2	0.5	-0.2	0.7
	Athe_1943	Calkro_0749	275-277	SLH-SLH	-0.5	-0.2	-0.2	0.0	-0.1	0.1
	Athe_2303	Calkro_0333	1013-1026	SLH	5.7	5.7	0.0	6.5	7.2	-0.7
	Athe_2341	Calkro_0210	483-484	SLH-SLH	0.1	0.3	-0.2	0.6	0.2	0.4
	Athe_2342	Calkro_0209	1003-1010	SLH	-0.9	-1.0	0.2	1.1	0.8	0.3
	Athe_1839	Calkro_0875	575-576	SLH-SLH-SLH	-0.5	4.5	-5.0	-0.7	0.1	-0.8
	Athe_2295	Calkro_0339	1074-1075	SLH-SLH	-0.4	0.3	-0.7	0.1	0.5	-0.3
	Athe_0077		1710	SLH-SLH-SLH-Big1-Tglut	2.8	3.2	-0.4			
	Athe_0608	Calkro_2018	547	SLH-SLH-SLH	-1.0	-1.5	0.5	-1.6	-1.4	-0.2
		Calkro_0360	793-798	SLH-SLH-SLH				2.7	2.9	-0.2
		Calkro_0197	1052	SLH-SLH				1.4	0.8	0.6
		Calkro_0155	549	MG2-SLH-SLH-SLH				-1.5	-0.7	-0.8
		Calkro_0090	664	SLH-SLH-SLH				-1.5	-1.1	-0.4
	Athe_0012	Calkro_0014	3027-2994	SLH-SLH-FN3-vWFA-SH3-RHSrep-RHScore	2.8	3.5	-0.6	2.8	2.0	0.8
	Athe_2223		591	SLH	-1.8	-1.7	-0.2			



FIGURE 5. Transcriptional response of genes encoding SLH domain proteins from *C. bescii* and *C. kronotskyensis*. Shown is the log squared mean (LSM) transcriptomic level of the 19 SLH domain proteins from *C. kronotskyensis* and 12 SLH domain proteins from *C. bescii* when each species is grown on crystalline cellulose (Avicel) and switchgrass (SWG). A log squared mean value of 0 represents average transcript abundance (black). Genes transcribed at levels higher than average have positive log squared mean values (red), whereas genes transcribed at levels lower than average have negative log squared mean values (green). Differential transcription is shown as Avicel minus switchgrass with negative values (orange) up-regulated on switchgrass relative to Avicel. Positive values (blue) are up-regulated on Avicel relative to switchgrass. Analysis is based on whole-genome oligonucleotide microarray experiments deposited in the NCBI Gene Expression Omnibus database with accession number GSE68810 (70). *Big*, bacterial immunoglobulin-like (CL0159); *Tglut*, transglutaminase-like superfamily (pfam01841); *MG2*, macroglobulin 2 (pfam01835); *vWFA*, von Willebrand factor type A (pfam00092); *SH3*, bacterial Src homology 3 (pfam08239); *RHSrep*, RHS repeat (pfam05593); *RHScore*, RHS-associated core domain (TIGR03696). *, Calkro_0121 is truncated after the first CBM32.

Manipulation of the *C. bescii* S-layer by the Insertion (Knock-in) of the Gene Encoding Calkro_0402—Because Calkro_0402 is very highly transcribed in *C. kronotskyensis* (Fig. 5) and utilized by a variety of xylan-degrading bacteria (Fig. 4A), Calkro_0402 was “knocked in” to genetically tractable *C. bescii* to examine its potential contribution to plant biomass degradation *in vivo*. *C. bescii* is a good genetic background for testing SLH proteins *in vivo*, because it produces only 12 SLH domain proteins in total and does not produce a homolog of Calkro_0402. Calkro_0402 was inserted into *C. bescii* uracil auxotroph strain JWCB018 using *pyrF* complementation and 5-fluoroarotic acid counterselection. The knock-in construct contained Calkro_0402, including the native signal peptide and the native predicted terminator sequence from *C. kronotskyensis*, under the control of the *slp* promoter from the main SLP (Athe_2303) in *C. bescii* (Fig. 6, A and B). As shown in Fig. 5, the main SLP (Athe_2303) is very highly and constitutively transcribed. Thus, its promoter should direct very high levels of transcription of Calkro_0402 in the knock-in construct. The knock-in was targeted at the $\Delta CbeI$ (Athe_2438) deletion locus in *C. bescii* strain JWCB018, because genetic manipulation in this area of the genome was successful previously (64). The PCR amplicon for the knock-in *C. bescii* strain RKCB103 compared with strain JWCB018 is shown in Fig. 6C.

Using this Calkro_0402 knock-in *C. bescii* strain RKCB103, immunofluorescence microscopy was performed to investigate

the expression of Calkro_0402 within the S-layer of *C. bescii*. For comparison, immunofluorescence microscopy was also performed on parent *C. bescii* strain JWCB018 and *C. kronotskyensis*, in addition to *C. bescii* strain RKCB103 (Fig. 6, D–F). *C. bescii* strain JWCB018, which does not have Calkro_0402, had minimal labeling with the anti-Calkro_0402 antibodies (Fig. 6D), whereas *C. bescii* strain RKCB103 was extensively labeled on the cell surface (Fig. 6F). Labeling of the native expression of Calkro_0402 in *C. kronotskyensis* is also shown (Fig. 6E). Based on transcription levels of Calkro_0402 and Athe_2303, the main SLP, (Fig. 5), the Calkro_0402 transcript in *C. bescii* strain RKCB103 should be >10-fold higher, using the *slp* promoter, compared with levels observed in wild-type *C. kronotskyensis*. This clearly relates to an increase in Calkro_0402 protein expression in *C. bescii* strain RKCB103 compared with native expression in *C. kronotskyensis*, as seen via the immunofluorescent labeling. Also of particular note is that the native signal peptide from *C. kronotskyensis* on Calkro_0402 appeared to function in *C. bescii* to route the protein for secretion. The *C. bescii*-produced Calkro_0402 also localized to the surface of the *C. bescii* strain RKCB103 cells and in Fig. 6F appears to localize primarily at the poles of the cell. The organization of SLH proteins on the cell surface is generally thought to be coordinated in bacteria that produce multiple SLH proteins, but the mechanisms by which this occurs have not been determined (82). This is the first example of manipu-

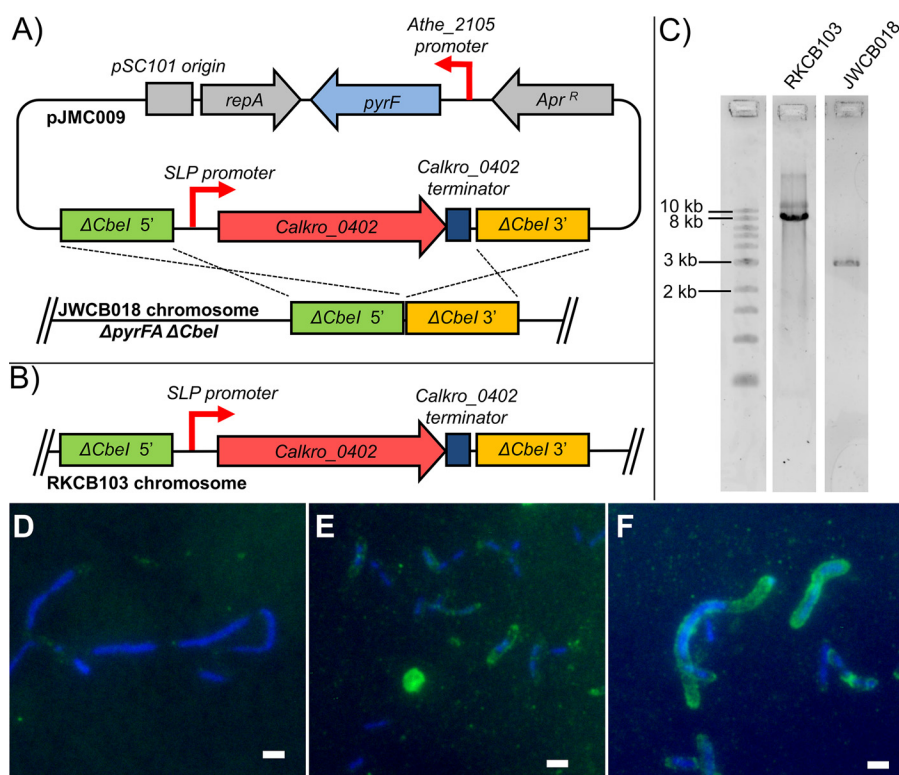


FIGURE 6. Construction of Calkro_0402 knock-in *C. bescii* strain RKCB103. A, Calkro_0402 knock-in vector pJMC009 homologous recombination with the chromosome of parent *C. bescii* strain JWCB018. pJMC009 was constructed using the pDCW121 (65) vector backbone, which contains the pSC101 origin, repA, and apramycin resistance marker for maintenance in *E. coli* as well as *C. bescii* wild type *pyrF* under the control of the *Athe_2105* promoter for selection of uracil prototrophy and 5-fluoroarotic acid counterselection. Cross-over regions 1 kb in length 5' and 3' to the $\Delta Cbel$ locus ($\Delta Athe_2438$) in strain JWCB018 were used to target Calkro_0402 for insertion via homologous recombination to that locus. The Calkro_0402 insertion construct included Calkro_0402 and an additional 81 bp downstream of the gene to include its predicted transcriptional terminator element amplified from *C. kronotskyensis* genomic DNA. High, constitutive expression of Calkro_0402 was driven by the 200-bp promoter element upstream of the *C. bescii* main SLP gene (*Athe_2303*). B, the Calkro_0402 construct is inserted in the chromosome of RKCB103 after first crossover vector integration and second crossover 5-fluoroarotic acid counterselection to remove the vector backbone containing *pyrF*. C, using primers outside of the 5' and 3' crossover regions (Table 1, $\Delta Athe_2438$ locus F and R), the $\Delta Cbel$ locus was amplified and sequenced to verify the Calkro_0402 knock-in. Strain JWCB018 has the expected 2.9-kb product, whereas strain RKCB103 has the expected 8.2-kb product with the 5.3-kb insertion of the SLP promoter and Calkro_0402 construct. A New England Biolabs 1-kb ladder was run alongside these PCR products. D–F, anti-Calkro_0402 immunofluorescence microscopy of *C. bescii* strain JWCB018, *C. kronotskyensis*, and *C. bescii* strain RKCB103 grown on birchwood xylan. D, *C. bescii* strain JWCB018, the genetic parent strain, which does not contain Calkro_0402, shows minimal labeling with the anti-Calkro_0402 antibodies. E and F, Calkro_0402 is shown localized on the cell surface in both *C. kronotskyensis* and *C. bescii* strain RKCB103 and appears primarily at the poles of the cells. All cells are labeled with chicken anti-Calkro_0402 total IgY primary antibody and DyLight 488-conjugated goat anti-chicken secondary antibody (green) with DAPI as a counterstain (blue). Scale bars, 2 μ m.

lation of the *Caldicellulosiruptor* S-layer through genetic modification.

***C. bescii* Strain RKCB103 Xylan Solubilization**—To understand the role of Calkro_0402 *in vivo*, the ability of *C. bescii* strains RKCB103 and JWCB018 to solubilize plant biomass in culture was examined. Fig. 7A shows the solubilization of oat spelt and birchwood xyans. Strain RKCB103 is able to solubilize significantly more washed oat spelt xylan than strain JWCB018; the xylose equivalents from the soluble xylooligosaccharides measured in the supernatant are more than double for strain RKCB103 compared with strain JWCB018 (Fig. 7B). For both the washed and unwashed birch xylan substrates, strain RKCB103 performed slightly better and released more xylose equivalents to the supernatant than strain JWCB018. Other biomass substrates tested (diluted acid-pretreated *P. trichocarpa* \times *P. deltoides*, dilute acid-pretreated switchgrass, and unpretreated *Panicum virgatum* switchgrass) showed no significant difference in solubilization and also showed <30 μ g/ml xylose equivalents in the culture supernatant (data not shown). This suggests that on these lignocellulosic substrates, *C. bescii*

strain JWCB018 produced enough xylanase activity to remove xylan at the rate at which it was exposed from the complex polysaccharide matrix in the substrate, and cellulose solubilization or occlusion of the polysaccharides by lignins was probably limiting the overall solubilization. However, in the substrates with high xylan content, strain RKCB103 with the addition of Calkro_0402 outperformed strain JWCB018.

Immunofluorescence microscopy (Fig. 6F) shows that Calkro_0402 is localized on the surface of strain RKCB103 cells. While the enzyme is tethered to the cell surface, the GH and CBM domains of Calkro_0402 interact with the xylan substrate. This suggests that Calkro_0402 plays a role in mediating cell attachment to xylan substrates. Cultures of strain JWCB018 and strain RKCB103 (Fig. 7, C and D, respectively) grown on washed birchwood xylan support this role for Calkro_0402. These cultures contained approximately the same number of cells as determined by cell counts (data not shown), but the supernatant in Fig. 7D for strain RKCB103 with Calkro_0402 is relatively clear, because the cells appear to be attached to the insoluble xylan at the bottom of the culture bottle. The strain

C. kronotskyensis SLH Glycoside Hydrolases

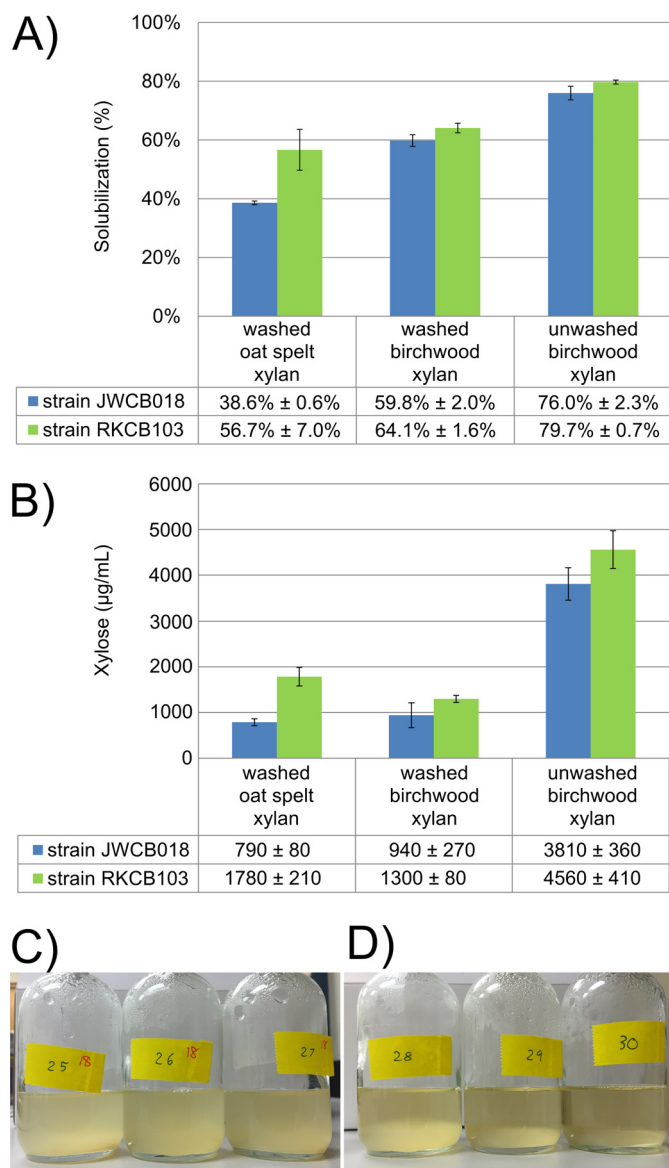


FIGURE 7. Increased xylan solubilization and xylan attachment by Calkro_0402 knock-in *C. bescii* strain RKCB103. A, total biomass solubilization of washed oat spelt xylan, washed birchwood xylan, and unwashed birchwood xylan after 45.5 h of growth of *C. bescii* strain JWCB018 or RKCB103. B, xylose measured in the acid-hydrolyzed culture supernatant harvested at 45.5 h. Error bars, S.D. ($n = 3$). C, *C. bescii* strain JWCB018 cultures on washed birchwood xylan appear very turbid (C), and *C. bescii* strain RKCB103 cultures appear much less turbid (D) while having the same cell density/ml of culture. C, *C. bescii* strain RKCB103 appears to be more readily attached to the insoluble washed birchwood xylan substrate, suggesting that the expression of Calkro_0402 in this strain is playing a role in tethering the cells to the xylan substrate.

JWCB018 cultures (Fig. 7C) were more turbid, suggesting that the cells did not as readily attach to the biomass substrate.

To understand the role of Calkro_0402 in improved xylan solubilization, a time course experiment was performed on washed oat spelt xylan. Fig. 8A shows the planktonic cell density for strains JWCB018 and RKCB103 over the duration of the culture. The cell densities of the two strains track each other closely. When monitoring xylose release, roughly 9–12 h postinoculation, the xylose hydrolyzed from xylooligosaccharides by strain RKCB103 was measurable above the baseline abiotic control, whereas strain JWCB018 took between 16 and 22 h

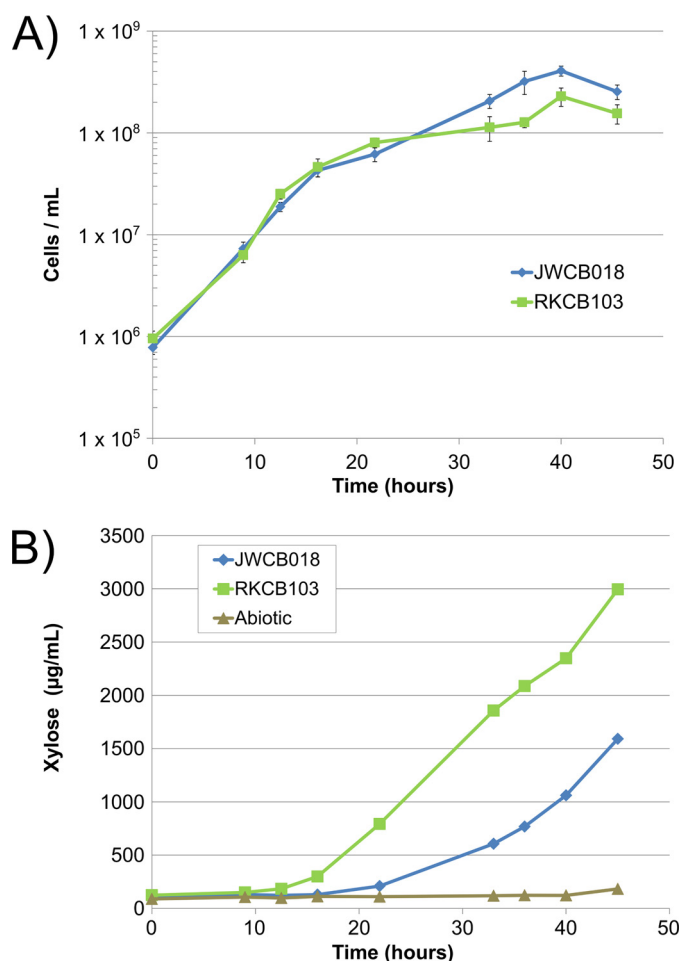


FIGURE 8. Time course of washed oat spelt xylan solubilization. A, cell densities of *C. bescii* strains JWCB018 (blue) and RKCB103 (green) over time while growing on washed oat spelt xylan. B, xylose measured in acid-hydrolyzed supernatant samples for *C. bescii* strains JWCB018 (blue) and RKCB103 (green) and an abiotic control (brown) (B). Error bars, S.D.

postinoculation (Fig. 8B). It is important to note that the strains were consuming xylose as they degraded the xylan substrate, and these values represent the xylose from excess xylooligosaccharides released by the enzymatic action of the cells that has not been consumed for growth. As with the closed bottle total solubilization experiment, strain RKCB103 has about double the xylose equivalents in the supernatant samples as strain JWCB018 at 45.5 h, the point at which the cultures were harvested.

Discussion

Catalytic CAZyme-containing SLH domain proteins are produced by a variety of lignocellulose-degrading bacteria (21, 22, 45). The genomes of 12 *Caldicellulosiruptor* species encode eight different groups of these (Fig. 1), a subset of the 34 groups of *Caldicellulosiruptor* SLH domain proteins (supplemental Table S1). These proteins are one of several mechanisms by which *Caldicellulosiruptor* species effect plant biomass degradation (21, 59, 61–63).

Calkro_0111 from *C. kronotskyensis* is the largest glycoside hydrolase from all of the biomass degradation enzymes in the *Caldicellulosiruptor* genus, free or cell-associated, and is

entirely unique to *C. kronotskyensis*. The GH16 domain of Calkro_0111 is an endoglucanase, whereas the GH55 is an exoglucanase (Fig. 3). Thus, the two GH domains probably work synergistically, as has been shown for other *Caldicellulosiruptor* enzymes without SLH domains but with two catalytic domains (76, 79, 80). Various truncation mutants of Calkro_0111 (Fig. 3D) were examined, revealing that the non-catalytic ACL domain adjacent to the GH16 domain is necessary for full activity. Furthermore, for the GH55 domain of Calkro_0111, both the ACL-FN3-FN3 domain grouping and two CBM32 domains improved the activity of the GH55 domain.

The very large multidomain structure of Calkro_0111 is characteristic of many *Caldicellulosiruptor* polysaccharide-degrading enzymes, where this architecture is thought to have arisen from domain shuffling (83, 84). Specifically, for Calkro_0111, the N terminus GH16 portion is similar to the N terminus of Calkro_0072 (45% amino acid identity), and the C terminus GH55 portion is similar to Calkro_0113 (58% amino acid identity). These protein segments may have combined by domain shuffling to form Calkro_0111. However, the ACL-FN3-FN3-ACL-FN3-FN3 motif in the middle of Calkro_0111 and in homolog Calkro_0121 is completely unique to these two genes. These ACL domains belong to the same protein superfamily (CL22458 RICIN superfamily) as fascins, which play a role in bundling actin filaments for cell adhesion and migration in *Drosophila* and vertebrate species (85). Plants and brown algae, such as *Laminaria* sp., produce actin and actin bundling proteins that are distinct from fascins for a variety of cellular roles (86, 87). The ACL domains of Calkro_0111 may play a role in attachment of this enzyme to actin found in algal or plant cells, similar to the role of a CBM for carbohydrate binding, to help localize the enzyme to laminarin-containing substrates.

Many GH16- and GH55-containing enzymes are active on β -1,3-glucans. Calkro_0111 activity was detected on a model substrate, laminarin (β -1,3-1,6-glucan), albeit at modest levels such that this is not likely to be its natural substrate. In fact, β -1,3-glucans, similar to laminarin, are produced in plant reproductive and wound tissue (callose) (88, 89), exopolysaccharide from bacteria (curdian) (90), algae such as *L. digitata* (laminarin), and lichen such as *Certraria islandica* (lichenan). In addition to this unique substrate preference of Calkro_0111, its genomic neighborhood is also unique, containing other extracellular biomass-degrading enzymes that have no homologs within other species in the genus. These include GH16/GH55 Calkro_0121, GH55 Calkro_0113, and GH81 Calkro_0114. This locus also encodes two ABC transporters, one of which is homologous to a putative glucooligosaccharide transporter in *C. saccharolyticus* (91). This entire genomic region is transcribed at relatively low levels when *C. kronotskyensis* is grown on Avicel or switchgrass. Taken together, this genomic locus, including Calkro_0111, probably degrades unique β -1,3-glucans from lichens, algae, or other microorganisms that may be more abundant in the natural environment of Kamchatka, Russia, from which *C. kronotskyensis* was isolated.

The large size of the gene encoding Calkro_0111 demonstrates that this unique multidomain arrangement is beneficial to *C. kronotskyensis* for it to be maintained and even duplicated as Calkro_0121. More broadly in the genus *Caldicellulosirup-*

tor, the unique multidomain architecture of enzymes, both with and without SLH domains, has probably evolved to appropriately space the CAZyme domains for increased synergy and activity. Specifically, for SLH domain proteins, domain spacing must also accommodate the tethering of the SLH domains at one end of the protein to the cell surface while it is attaching to and degrading the plant biomass substrate with the other. The large size of these catalytic SLH proteins may reflect the length needed to swing out away from the cell to reach biomass substrates to which they can attach. Although domain spacing and arrangement appear to be critical factors in the activity of Calkro_0111, no pattern for domain arrangement through all of the catalytic *Caldicellulosiruptor* SLH proteins is readily apparent, based on amino acid sequence. Lacking structural data, which are difficult to obtain for these large multidomain proteins, the orientation of each domain relative to another cannot be determined precisely. It does seem likely, however, that each protein has evolved its domain spacing to enable its unique combination of binding and catalytic domains to function properly while being tethered to the cell.

Whereas Calkro_0111 and Calkro_0121 are transcribed at low levels when grown on plant biomass substrates, all of the other SLH GH and PL enzymes from *C. kronotskyensis* and *C. bescii* are up-regulated when these species are grown on switchgrass compared with Avicel (Fig. 5), including the xylanase Calkro_0402. This suggests an important role in plant biomass degradation. Calkro_0402 belongs to a large group of homologous CBM22/GH10/CBM9 xylanases (Fig. 4A). While Calkro_0402 releases primarily xylobiose and xylotriose from birchwood xylan (Fig. 4E), similar to previously characterized homologs (28, 31), the optimal temperature of 80 °C for Calkro_0402 (Fig. 4D) makes it one of the most thermophilic versions of this family of xylanase enzymes characterized to date. As is predicted by the presence of SLH domains, Calkro_0402 is localized to the cell surface of *C. kronotskyensis* (Fig. 2, D and E), which is a common feature of many homologs of Calkro_0402, including some shown in Fig. 4A associated with the cell by means other than SLH domains. The Calkro_0402 homolog from *Thermotoga maritima* (and presumably homologs in other *Thermotoga* sp.) is cell-associated by an N-terminal hydrophobic peptide anchor and not SLH domains (92). Furthermore, the *Clostridium clariflavum* xylanase lacks SLH domains but has a dockerin domain on its C terminus, which would allow this enzyme to associate via protein-protein interactions into a cellulosome multienzyme complex that is also typically anchored to the cell surface via SLH domains (61). The fact that these homologs without SLH domains can remain associated with the cell implies that there is particular utility for having this type of CBM22/GH10/CBM9 xylanase associated with the cell.

Using genetic manipulation of *C. bescii* to knock in Calkro_0402, the role of this SLH protein *in vivo* for substrate attachment (Fig. 7, C and D) and degradation (Figs. 7 (A and B) and 8 (A and B)) could be examined. Wild-type *C. bescii* has previously been shown to attach to xylan substrates (63). Our observations suggest that modification of the *C. bescii* S-layer to contain SLH domain xylanase Calkro_0402 probably improves this attachment (Fig. 7, C and D). Truncation mutants

C. kronotskyensis SLH Glycoside Hydrolases

of Xyn10B from *Clostridium stercorarium* and Xyn10A from *Clostridium josui* showed that the CBM9 and CBM22 domains mediate the attachment of these enzymes to xylan and other substrates (42, 43). While these two xylanases are phylogenetically distant from Calkro_0402 (Fig. 4A), the role of these CBM22 and CBM9 domains is probably very similar in Calkro_0402 in the functional role of degrading xylan substrates. The attachment of the Calkro_0402 knock-in strain RKCB103 is also probably a significant factor in its improved solubilization of xylans (Fig. 7A). Both *C. bescii* and *C. kronotskyensis* produce at least five other extracellular xylanases targeted for the secretome with GH10, GH11, or GH43 domains. If the cell is attached to xylan by Calkro_0402, these enzymes are secreted from the cell proximate to their substrate, probably making them more effective in the degradation process as well.

Very few of the diverse catalytic CAZyme-containing SLH domain proteins have been characterized, but their role in biomass deconstruction clearly merits closer examination. There are more than 20,000 SLH domain-containing proteins predicted in over 1,800 microbial genomes. These unusual proteins on the surface of bacterial cells contain a variety of functional protein domains, localized at the interface between the cell and its environment. Although a full understanding of bacterial S-layer proteins and their varied and important roles at the cell surface is not yet available, the results reported here provide new insights into the role of SLH GHs as agents of plant polysaccharide degradation.

Author Contributions—J. M. C., W. S. P., G. W. H., A. L. T., and S. E. B.-S. contributed to protein cloning, expression, and enzymatic characterization. J. M. C., W. S. P., J. H. L., J. H. W., L. L. L., and S. E. B.-S. contributed to construction of strain RKCB103. J. M. C., G. W. H., and S. E. B.-S. contributed to microscopy. J. M. C., J. H. L., G. W. H., and J. V. Z. contributed to biomass solubilization assays and HPLC analysis. J. M. C. and R. M. K. designed and directed the research and drafted the manuscript. All authors provided comments on and approved the final manuscript.

Acknowledgments—We acknowledge the North Carolina State University Cellular and Molecular Imaging Facility and Dr. Eva Johannes for assistance in operating the Zeiss LSM 710 confocal microscope.

References

1. Sára, M., and Sleytr, U. B. (2000) S-Layer proteins. *J. Bacteriol.* **182**, 859–868
2. Sleytr, U. B., and Beveridge, T. J. (1999) Bacterial S-layers. *Trends Microbiol.* **7**, 253–260
3. Albers, S.-V., and Meyer, B. H. (2011) The archaeal cell envelope. *Nat. Rev. Microbiol.* **9**, 414–426
4. Kern, J., Wilton, R., Zhang, R., Binkowski, T. A., Joachimiak, A., and Schneewind, O. (2011) Structure of surface layer homology (SLH) domains from *Bacillus anthracis* surface array protein. *J. Biol. Chem.* **286**, 26042–26049
5. Mesnage, S., Fontaine, T., Mignot, T., Delepierre, M., Mock, M., and Fouet, A. (2000) Bacterial SLH domain proteins are non-covalently anchored to the cell surface via a conserved mechanism involving wall polysaccharide pyruvylation. *EMBO J.* **19**, 4473–4484
6. Fagan, R. P., Janoir, C., Collignon, A., Mastrantonio, P., Poxton, I. R., and

- Fairweather, N. F. (2011) A proposed nomenclature for cell wall proteins of *Clostridium difficile*. *J. Med. Microbiol.* **60**, 1225–1228
7. Boot, H. J., Kolen, C. P., and Pouwels, P. H. (1995) Identification, cloning, and nucleotide sequence of a silent S-layer protein gene of *Lactobacillus acidophilus* ATCC 4356 which has extensive similarity with the S-layer protein gene of this species. *J. Bacteriol.* **177**, 7222–7230
8. Johnson, B. R., Hymes, J., Sanozy-Dawes, R., Henriksen, E. D., Barrangou, R., and Klaenhammer, T. R. (2015) Conserved S-layer-associated proteins revealed by exoproteomic survey of S-layer-forming lactobacilli. *Appl. Environ. Microbiol.* **82**, 134–145
9. Veith, A., Klingl, A., Zolghadr, B., Lauber, K., Mentele, R., Lottspeich, F., Rachel, R., Albers, S. V., and Kletzin, A. (2009) *Acidianus*, *Sulfolobus* and *Metallosphaera* surface layers: structure, composition and gene expression. *Mol. Microbiol.* **73**, 58–72
10. Abdul Halim, M. F., Pfeiffer, F., Zou, J., Frisch, A., Haft, D., Wu, S., Tolić, N., Brewer, H., Payne, S. H., Paša-Tolić, L., and Pohlschroder, M. (2013) *Haloferax volcanii* archaeosortase is required for motility, mating, and C-terminal processing of the S-layer glycoprotein. *Mol. Microbiol.* **88**, 1164–1175
11. Abdul Halim, M. F., Karch, K. R., Zhou, Y., Haft, D. H., Garcia, B. A., and Pohlschroder, M. (2015) Permuting the PGF-CTERM signature motif blocks both archaeosortase-dependent C-terminal cleavage and prenyl lipid attachment for the *Haloferax volcanii* S-layer glycoprotein. *J. Bacteriol.* 10.1128/JB.00849-15
12. Fagan, R. P., and Fairweather, N. F. (2014) Biogenesis and functions of bacterial S-layers. *Nat. Rev. Microbiol.* **12**, 211–222
13. Pham, T. K., Roy, S., Noirel, J., Douglas, L., Wright, P. C., and Stafford, G. P. (2010) A quantitative proteomic analysis of biofilm adaptation by the periodontal pathogen *Tannerella forsythia*. *Proteomics* **10**, 3130–3141
14. Honma, K., Inagaki, S., Okuda, K., Kuramitsu, H. K., and Sharma, A. (2007) Role of a *Tannerella forsythia* exopolysaccharide synthesis operon in biofilm development. *Microb. Pathog.* **42**, 156–166
15. Reynolds, C. B., Emerson, J. E., de la Riva, L., Fagan, R. P., and Fairweather, N. F. (2011) The *Clostridium difficile* cell wall protein CwpV is antigenically variable between strains, but exhibits conserved aggregation-promoting function. *PLoS Pathog.* **7**, e1002024
16. Sun, Z., Kong, J., Hu, S., Kong, W., Lu, W., and Liu, W. (2013) Characterization of a S-layer protein from *Lactobacillus crispatus* K313 and the domains responsible for binding to cell wall and adherence to collagen. *Appl. Microbiol. Biotechnol.* **97**, 1941–1952
17. de la Riva, L., Willing, S. E., Tate, E. W., and Fairweather, N. F. (2011) Roles of cysteine proteases Cwp84 and Cwp13 in biogenesis of the cell wall of *Clostridium difficile*. *J. Bacteriol.* **193**, 3276–3285
18. Anderson, V. J., Kern, J. W., McCool, J. W., Schneewind, O., and Missiakas, D. (2011) The SLH-domain protein BslO is a determinant of *Bacillus anthracis* chain length. *Mol. Microbiol.* **81**, 192–205
19. Brahamsha, B. (1996) An abundant cell-surface polypeptide is required for swimming by the nonflagellated marine cyanobacterium *Synechococcus*. *Proc. Natl. Acad. Sci. U.S.A.* **93**, 6504–6509
20. McCarren, J., and Brahamsha, B. (2007) SwmB, a 1.12-megadalton protein that is required for nonflagellar swimming motility in *Synechococcus*. *J. Bacteriol.* **189**, 1158–1162
21. Ozdemir, I., Blumer-Schuette, S. E., and Kelly, R. M. (2012) S-layer homology domain proteins Csc_0678 and Csc_2722 are implicated in plant polysaccharide deconstruction by the extremely thermophilic bacterium *Caldicellulosiruptor saccharolyticus*. *Appl. Environ. Microbiol.* **78**, 768–777
22. Egelseer, E., Schocher, I., Sára, M., and Sleytr, U. B. (1995) The S-layer from *Bacillus stearothermophilus* DSM 2358 functions as an adhesion site for a high-molecular-weight amylase. *J. Bacteriol.* **177**, 1444–1451
23. Lombard, V., Golaconda Ramulu, H., Drula, E., Coutinho, P. M., and Henrissat, B. (2014) The carbohydrate-active enzymes database (CAZy) in 2013. *Nucleic Acids Res.* **42**, D490–D495
24. Lemaire, M., Ohayon, H., Gounon, P., Fujino, T., and Béguin, P. (1995) OlpB, a new outer layer protein of *Clostridium thermocellum*, and binding of its S-layer-like domains to components of the cell envelope. *J. Bacteriol.* **177**, 2451–2459
25. Fujino, T., Béguin, P., and Aubert, J. P. (1993) Organization of a *Clostrid-*

- ium thermocellum* gene cluster encoding the cellulosomal scaffolding protein CipA and a protein possibly involved in attachment of the cellulosome to the cell surface. *J. Bacteriol.* **175**, 1891–1899
26. Fontes, C. M., and Gilbert, H. J. (2010) Cellulosomes: highly efficient nanomachines designed to deconstruct plant cell wall complex carbohydrates. *Annu. Rev. Biochem.* **79**, 655–681
 27. Markowitz, V. M., Chen, I. M., Palaniappan, K., Chu, K., Szeto, E., Pillay, M., Ratner, A., Huang, J., Woyke, T., Huntemann, M., Anderson, I., Billis, K., Varghese, N., Mavromatis, K., Pati, A., Ivanova, N. N., and Kyrpides, N. C. (2014) IMG 4 version of the integrated microbial genomes comparative analysis system. *Nucleic Acids Res.* **42**, D560–D567
 28. Han, Y., Agarwal, V., Dodd, D., Kim, J., Bae, B., Mackie, R. I., Nair, S. K., and Cann, I. K. (2012) Biochemical and structural insights into xylan utilization by the thermophilic bacterium *Caldanaerobius polysaccharolyticus*. *J. Biol. Chem.* **287**, 34946–34960
 29. Han, Y., Dodd, D., Hespden, C. W., Ohene-Adjei, S., Schroeder, C. M., Mackie, R. I., and Cann, I. K. (2010) Comparative analyses of two thermophilic enzymes exhibiting both β -1,4 mannosidic and β -1,4 glucosidic cleavage activities from *Caldanaerobius polysaccharolyticus*. *J. Bacteriol.* **192**, 4111–4121
 30. Lee, S. P., Morikawa, M., Takagi, M., and Imanaka, T. (1994) Cloning of the *aapT* gene and characterization of its product, α -amylase-pullulanase (AapT), from thermophilic and alkaliphilic *Bacillus* sp. strain XAL601. *Appl. Environ. Microbiol.* **60**, 3764–3773
 31. Waenonukul, R., Pason, P., Kyu, K. L., Sakka, K., Kosugi, A., Mori, Y., and Ratanakhanokchai, K. (2009) Cloning, sequencing, and expression of the gene encoding a multidomain endo- β -1,4-xylanase from *Paenibacillus curdlanolyticus* B-6, and characterization of the recombinant enzyme. *J. Microbiol. Biotechnol.* **19**, 277–285
 32. Cheng, Y. M., Hong, T. Y., Liu, C. C., and Meng, M. (2009) Cloning and functional characterization of a complex endo- β -1,3-glucanase from *Paenibacillus* sp. *Appl. Microbiol. Biotechnol.* **81**, 1051–1061
 33. Stjohn, F. J., Rice, J. D., and Preston, J. F. (2006) *Paenibacillus* sp. strain JDR-2 and XynA1: a novel system for methylglucuronoxylan utilization. *Appl. Environ. Microbiol.* **72**, 1496–1506
 34. Ito, Y., Tomita, T., Roy, N., Nakano, A., Sugawara-Tomita, N., Watanabe, S., Okai, N., Abe, N., and Kamio, Y. (2003) Cloning, expression, and cell surface localization of *Paenibacillus* sp. strain W-61 xylanase 5, a multidomain xylanase. *Appl. Environ. Microbiol.* **69**, 6969–6978
 35. Itoh, T., Sugimoto, I., Hibi, T., Suzuki, F., Matsuo, K., Fujii, Y., Taketo, A., and Kimoto, H. (2014) Overexpression, purification, and characterization of *Paenibacillus* cell surface-expressed chitinase ChiW with two catalytic domains. *Biosci. Biotechnol. Biochem.* **78**, 624–634
 36. St John, F. J., Preston, J. F., and Pozharski, E. (2012) Novel structural features of xylanase A1 from *Paenibacillus* sp. JDR-2. *J. Struct. Biol.* **180**, 303–311
 37. Kim, H., Jung, K. H., and Pack, M. Y. (2000) Molecular characterization of *xynX*, a gene encoding a multidomain xylanase with a thermostabilizing domain from *Clostridium thermocellum*. *Appl. Microbiol. Biotechnol.* **54**, 521–527
 38. Fuchs, K.-P., Zverlov, V. V., Velikodvorskaya, G. A., Lottspeich, F., and Schwarz, W. H. (2003) Lic16A of *Clostridium thermocellum*, a non-cellulosomal, highly complex endo- β -1,3-glucanase bound to the outer cell surface. *Microbiology* **149**, 1021–1031
 39. Adelsberger, H., Hertel, C., Glawischnig, E., Zverlov, V. V., and Schwarz, W. H. (2004) Enzyme system of *Clostridium stercorarium* for hydrolysis of arabinoxylan: reconstitution of the *in vivo* system from recombinant enzymes. *Microbiology* **150**, 2257–2266
 40. Feng, J. X., Karita, S., Fujino, E., Fujino, T., Kimura, T., Sakka, K., and Ohmiya, K. (2000) Cloning, sequencing, and expression of the gene encoding a cell-bound multi-domain xylanase from *Clostridium josui*, and characterization of the translated product. *Biosci. Biotechnol. Biochem.* **64**, 2614–2624
 41. Ali, M. K., Fukumura, M., Sakano, K., Karita, S., Kimura, T., Sakka, K., and Ohmiya, K. (1999) Cloning, sequencing, and expression of the gene encoding the *Clostridium stercorarium* xylanase C in *Escherichia coli*. *Biosci. Biotechnol. Biochem.* **63**, 1596–1604
 42. Ali, E., Araki, R., Zhao, G., Sakka, M., Karita, S., Kimura, T., and Sakka, K. (2005) Functions of family-22 carbohydrate-binding modules in *Clostridium josui* Xyn10A. *Biosci. Biotechnol. Biochem.* **69**, 2389–2394
 43. Ali, M. K., Hayashi, H., Karita, S., Goto, M., Kimura, T., Sakka, K., and Ohmiya, K. (2001) Importance of the carbohydrate-binding module of *Clostridium stercorarium* Xyn10B to xylan hydrolysis. *Biosci. Biotechnol. Biochem.* **65**, 41–47
 44. Ali, M. K., Kimura, T., Sakka, K., and Ohmiya, K. (2001) The multidomain xylanase Xyn10B as a cellulose-binding protein in *Clostridium stercorarium*. *FEMS Microbiol. Lett.* **198**, 79–83
 45. Brechtel, E., Matuschek, M., Hellberg, A., Egelseer, E. M., Schmid, R., and Bahl, H. (1999) Cell wall of *Thermoanaerobacterium thermosulfurigenes* EM1: isolation of its components and attachment of the xylanase XynA. *Arch. Microbiol.* **171**, 159–165
 46. Liu, S. Y., Gherardini, F. C., Matuschek, M., Bahl, H., and Wiegel, J. (1996) Cloning, sequencing, and expression of the gene encoding a large S-layer-associated endoxylanase from *Thermoanaerobacterium* sp. strain JW/SL-YS 485 in *Escherichia coli*. *J. Bacteriol.* **178**, 1539–1547
 47. Matuschek, M., Burchhardt, G., Sahm, K., and Bahl, H. (1994) Pullulanase of *Thermoanaerobacterium thermosulfurigenes* EM1 (*Clostridium thermosulfurogenes*): molecular analysis of the gene, composite structure of the enzyme, and a common model for its attachment to the cell surface. *J. Bacteriol.* **176**, 3295–3302
 48. Matuschek, M., Sahm, K., Zibat, A., and Bahl, H. (1996) Characterization of genes from *Thermoanaerobacterium thermosulfurigenes* EM1 that encode two glycosyl hydrolases with conserved S-layer-like domains. *Mol. Gen. Genet.* **252**, 493–496
 49. Shao, W., Deblouis, S., and Wiegel, J. (1995) A high-molecular-weight, cell-associated xylanase isolated from exponentially growing *Thermoanaerobacterium* sp. strain JW/SL-YS485. *Appl. Environ. Microbiol.* **61**, 937–940
 50. Huang, X., Li, Z., Du, C., Wang, J., and Li, S. (2015) Improved expression and characterization of a multidomain xylanase from *Thermoanaerobacterium aotearoense* SCUT27 in *Bacillus subtilis*. *J. Agric. Food Chem.* **63**, 6430–6439
 51. Hung, K. S., Liu, S. M., Fang, T. Y., Tzou, W. S., Lin, F. P., Sun, K. H., and Tang, S. J. (2011) Characterization of a salt-tolerant xylanase from *Thermoanaerobacterium saccharolyticum* NTOU1. *Biotechnol. Lett.* **33**, 1441–1447
 52. Morris, D. D., Gibbs, M. D., Ford, M., Thomas, J., and Bergquist, P. L. (1999) Family 10 and 11 xylanase genes from *Caldicellulosiruptor* sp. strain Rt69B. *1. Extremophiles* **3**, 103–111
 53. Blumer-Schuetz, S. E., Ozdemir, I., Mistry, D., Lucas, S., Lapidus, A., Cheng, J.-F., Goodwin, L. A., Pitluck, S., Land, M. L., Hauser, L. J., Woyke, T., Mikhailova, N., Pati, A., Kyrpides, N. C., Ivanova, N., Detter, J. C., Walston-Davenport, K., Han, S., Adams, M. W. W., and Kelly, R. M. (2011) Complete genome sequences for the anaerobic, extremely thermophilic plant biomass-degrading bacteria *Caldicellulosiruptor hydrothermalis*, *Caldicellulosiruptor kristjanssonii*, *Caldicellulosiruptor kronotskyensis*, *Caldicellulosiruptor owensensis*, and *Caldicellulosiruptor lactoaceticus*. *J. Bacteriol.* **193**, 1483–1484
 54. Lee, L. L., Izquierdo, J. A., Blumer-Schuetz, S. E., Zurawski, J. V., Conway, J. M., Cottingham, R. W., Huntemann, M., Copeland, A., Chen, I. M., Kyrpides, N., Markowitz, V., Palaniappan, K., Ivanova, N., Mikhailova, N., Ovchinnikova, G., Andersen, E., Pati, A., Stamatis, D., Reddy, T. B., Shapiro, N., Nordberg, H. P., Cantor, M. N., Hua, S. X., Woyke, T., and Kelly, R. M. (2015) Complete genome sequences of *Caldicellulosiruptor* sp. Strain Rt8.B8, *Caldicellulosiruptor* sp. Strain Wai35.B1, and “*Thermoanaerobacter cellulolyticus*”. *Genome Announc.* **10**.1128/genomeA.00440–15
 55. Elkins, J. G., Lochner, A., Hamilton-Brehm, S. D., Davenport, K. W., Podar, M., Brown, S. D., Land, M. L., Hauser, L. J., Klingeman, D. M., Raman, B., Goodwin, L. A., Tapia, R., Meincke, L. J., Detter, J. C., Bruce, D. C., Han, C. S., Palumbo, A. V., Cottingham, R. W., Keller, M., and Graham, D. E. (2010) Complete genome sequence of the cellulolytic thermophile *Caldicellulosiruptor obsidiansis* OB47T. *J. Bacteriol.* **192**, 6099–6100
 56. van de Werken, H. J., Verhaart, M. R., VanFossen, A. L., Willquist, K., Lewis, D. L., Nichols, J. D., Goorissen, H. P., Mongodin, E. F., Nelson, K. E.,

- van Niel, E. W., Stams, A. J., Ward, D. E., de Vos, W. M., van der Oost, J., Kelly, R. M., and Kengen, S. W. (2008) Hydrogenomics of the extremely thermophilic bacterium *Caldicellulosiruptor saccharolyticus*. *Appl. Environ. Microbiol.* **74**, 6720–6729
57. Kataeva, I. A., Yang, S. J., Dam, P., Poole, F. L., 2nd, Yin, Y., Zhou, F., Chou, W. C., Xu, Y., Goodwin, L., Sims, D. R., Detter, J. C., Hauser, L. J., Westpheling, J., and Adams, M. W. (2009) Genome sequence of the anaerobic, thermophilic, and cellulolytic bacterium “*Anaerocellum thermophilum*” DSM 6725. *J. Bacteriol.* **191**, 3760–3761
58. Conway, J. M., Zurawski, J. V., Lee, L. L., Blumer-Schuetz, S. E., and Kelly, R. M. (2015) in *Thermophilic Microorganisms* (Li, F., ed) pp. 91–120, Caister Academic Press, Norfolk, UK
59. Blumer-Schuetz, S. E., Giannone, R. J., Zurawski, J. V., Ozdemir, I., Ma, Q., Yin, Y., Xu, Y., Kataeva, I., Poole, F. L., 2nd, Adams, M. W., Hamilton-Brehm, S. D., Elkins, J. G., Larimer, F. W., Land, M. L., Hauser, L. J., Cottingham, R. W., Hettich, R. L., and Kelly, R. M. (2012) *Caldicellulosiruptor* core and pangenome reveal determinants for noncellulosomal thermophilic deconstruction of plant biomass. *J. Bacteriol.* **194**, 4015–4028
60. Blumer-Schuetz, S. E., Lewis, D. L., and Kelly, R. M. (2010) Phylogenetic, microbiological, and glycoside hydrolase diversities within the extremely thermophilic, plant biomass-degrading genus *Caldicellulosiruptor*. *Appl. Environ. Microbiol.* **76**, 8084–8092
61. Blumer-Schuetz, S. E., Brown, S. D., Sander, K. B., Bayer, E. A., Kataeva, I., Zurawski, J. V., Conway, J. M., Adams, M. W. W., and Kelly, R. M. (2014) Thermophilic lignocellulose deconstruction. *FEMS Microbiol. Rev.* **38**, 393–448
62. Blumer-Schuetz, S. E., Alahuhta, M., Conway, J. M., Lee, L. L., Zurawski, J. V., Giannone, R. J., Hettich, R. L., Lunin, V. V., Himmel, M. E., and Kelly, R. M. (2015) Discrete and structurally unique proteins (täpirins) mediate attachment of extremely thermophilic *Caldicellulosiruptor* species to cellulose. *J. Biol. Chem.* **290**, 10645–10656
63. Dam, P., Kataeva, I., Yang, S. J., Zhou, F., Yin, Y., Chou, W., Poole, F. L., 2nd, Westpheling, J., Hettich, R., Giannone, R., Lewis, D. L., Kelly, R., Gilbert, H. J., Henrissat, B., Xu, Y., and Adams, M. W. (2011) Insights into plant biomass conversion from the genome of the anaerobic thermophilic bacterium *Caldicellulosiruptor bescii* DSM 6725. *Nucleic Acids Res.* **39**, 3240–3254
64. Chung, D., Farkas, J., and Westpheling, J. (2013) Overcoming restriction as a barrier to DNA transformation in *Caldicellulosiruptor* species results in efficient marker replacement. *Biotechnol. Biofuels* **6**, 82
65. Cha, M., Chung, D., Elkins, J. G., Guss, A. M., and Westpheling, J. (2013) Metabolic engineering of *Caldicellulosiruptor bescii* yields increased hydrogen production from lignocellulosic biomass. *Biotechnol. Biofuels* **6**, 85
66. Gibson, D. G. (2011) Enzymatic assembly of overlapping DNA fragments. *Methods Enzymol.* **498**, 349–361
67. Studier, F. W. (2005) Protein production by auto-induction in high density shaking cultures. *Protein Expr. Purif.* **41**, 207–234
68. Geslin, C., Le Romancer, M., Erauso, G., Gaillard, M., Perrot, G., and Prieur, D. (2003) PAV1, the first virus-like particle isolated from a hyperthermophilic euryarchaeote, “*Pyrococcus abyssi*”. *J. Bacteriol.* **185**, 3888–3894
69. Farkas, J., Chung, D., Cha, M., Copeland, J., Grayeski, P., and Westpheling, J. (2013) Improved growth media and culture techniques for genetic analysis and assessment of biomass utilization by *Caldicellulosiruptor bescii*. *J. Ind. Microbiol. Biotechnol.* **40**, 41–49
70. Zurawski, J. V., Conway, J. M., Lee, L. L., Simpson, H. J., Izquierdo, J. A., Blumer-Schuetz, S., Nookaew, I., Adams, M. W. W., and Kelly, R. M. (2015) Comparative analysis of extremely thermophilic *Caldicellulosiruptor* species reveals common and differentiating cellular strategies for plant biomass utilization. *Appl. Environ. Microbiol.* **81**, 7159–7170
71. Petersen, T. N., Brunak, S., von Heijne, G., and Nielsen, H. (2011) SignalP 4.0: discriminating signal peptides from transmembrane regions. *Nat. Methods* **8**, 785–786
72. Ghose, T. K. (1987) Measurement of cellulase activities. *Pure Appl. Chem.* **59**, 257–268
73. Miller, G. L. (1959) Use of dinitrosalicylic acid reagent for determination of reducing sugar. *Anal. Chem.* **31**, 426–428
74. Xiao, Z., Storms, R., and Tsang, A. (2005) Microplate-based carboxymethylcellulose assay for endoglucanase activity. *Anal. Biochem.* **342**, 176–178
75. Xiao, Z., Storms, R., and Tsang, A. (2004) Microplate-based filter paper assay to measure total cellulase activity. *Biotechnol. Bioeng.* **88**, 832–837
76. VanFossen, A. L., Ozdemir, I., Zelin, S. L., and Kelly, R. M. (2011) Glycoside hydrolase inventory drives plant polysaccharide deconstruction by the extremely thermophilic bacterium *Caldicellulosiruptor saccharolyticus*. *Biotechnol. Bioeng.* **108**, 1559–1569
77. Lipscomb, G. L., Stirrett, K., Schut, G. J., Yang, F., Jenney, F. E., Jr., Scott, R. A., Adams, M. W., and Westpheling, J. (2011) Natural competence in the hyperthermophilic archaeon *Pyrococcus furiosus* facilitates genetic manipulation: construction of markerless deletions of genes encoding the two cytoplasmic hydrogenases. *Appl. Environ. Microbiol.* **77**, 2232–2238
78. Zhao, Y., Meng, K., Luo, H., Huang, H., Yuan, T., Yang, P., and Yao, B. (2013) Molecular and biochemical characterization of a new alkaline active multidomain xylanase from alkaline wastewater sludge. *World J. Microbiol. Biotechnol.* **29**, 327–334
79. Yi, Z., Su, X., Revindran, V., Mackie, R. I., and Cann, I. (2013) Molecular and biochemical analyses of CbCel9A/Cel48A, a highly secreted multimodular cellulase by *Caldicellulosiruptor bescii* during growth on crystalline cellulose. *PLoS One* **8**, e84172
80. Ye, L., Su, X., Schmitz, G. E., Moon, Y. H., Zhang, J., Mackie, R. I., and Cann, I. K. O. (2012) Molecular and biochemical analyses of the GH44 Module of CbMan5B/Cel44A, a bifunctional enzyme from the hyperthermophilic bacterium *Caldicellulosiruptor bescii*. *Appl. Environ. Microbiol.* **78**, 7048–7059
81. Brunecky, R., Alahuhta, M., Bomble, Y. J., Xu, Q., Baker, J. O., Ding, S. Y., Himmel, M. E., and Lunin, V. V. (2012) Structure and function of the *Clostridium thermocellum* cellobiohydrolase A X1-module repeat: enhancement through stabilization of the CbhA complex. *Acta Crystallogr. D Biol. Crystallogr.* **68**, 292–299
82. Schneewind, O., and Missiakas, D. M. (2012) Protein secretion and surface display in Gram-positive bacteria. *Philos. Trans. R. Soc. Lond. B Biol. Sci.* **367**, 1123–1139
83. Bergquist, P. L., Gibbs, M. D., Morris, D. D., Te’o, V. S. J., Saul, D. J., and Morgan, H. W. (1999) Molecular diversity of thermophilic cellulolytic and hemicellulolytic bacteria. *FEMS Microbiol. Ecol.* **28**, 99–110
84. Gibbs, M. D., Reeves, R. A., Farrington, G. K., Anderson, P., Williams, D. P., and Bergquist, P. L. (2000) Multidomain and multifunctional glycosyl hydrolases from the extreme thermophile *Caldicellulosiruptor* isolate Tok7B.1. *Curr. Microbiol.* **40**, 333–340
85. Kureishy, N., Sapountzi, V., Prag, S., Anilkumar, N., and Adams, J. C. (2002) Fascins, and their roles in cell structure and function. *Bioessays* **24**, 350–361
86. Thomas, C., Tholl, S., Moes, D., Dieterle, M., Papuga, J., Moreau, F., and Steinmetz, A. (2009) Actin bundling in plants. *Cell Motil. Cytoskeleton* **66**, 940–957
87. Charrier, B., Le Bail, A., and de Reviere, B. (2012) Plant proteus: brown algal morphological plasticity and underlying developmental mechanisms. *Trends Plant Sci.* **17**, 468–477
88. Verma, D. P., and Hong, Z. (2001) Plant callose synthase complexes. *Plant Mol. Biol.* **47**, 693–701
89. Dumas, C., and Knox, R. B. (1983) Callose and determination of pistil viability and incompatibility. *Theor. Appl. Genet.* **67**, 1–10
90. Harada, T. (1992) The story of research into curdlan and the bacteria producing it. *Trends Glycosci. Glycotechnol.* **4**, 309–317
91. Vanfossen, A. L., Verhaart, M. R., Kengen, S. M., and Kelly, R. M. (2009) Carbohydrate utilization patterns for the extremely thermophilic bacterium *Caldicellulosiruptor saccharolyticus* reveal broad growth substrate preferences. *Appl. Environ. Microbiol.* **75**, 7718–7724
92. Liebl, W., Winterhalter, C., Baumeister, W., Armbricht, M., and Valdez, M. (2008) Xylanase attachment to the cell wall of the hyperthermophilic bacterium *Thermotoga maritima*. *J. Bacteriol.* **190**, 1350–1358
93. Marchler-Bauer, A., Derbyshire, M. K., Gonzales, N. R., Lu, S., Chitsaz, F., Geer, L. Y., Geer, R. C., He, J., Gwadz, M., Hurwitz, D. I., Lanczycki, C. J.,

- Lu, F., Marchler, G. H., Song, J. S., Thanki, N., Wang, Z., Yamashita, R. A., Zhang, D., Zheng, C., and Bryant, S. H. (2015) CDD: NCBI's conserved domain database. *Nucleic Acids Res.* **43**, D222–D226
94. Punta, M., Coggill, P. C., Eberhardt, R. Y., Mistry, J., Tate, J., Boursnell, C., Pang, N., Forslund, K., Ceric, G., Clements, J., Heger, A., Holm, L., Sonnhammer, E. L., Eddy, S. R., Bateman, A., and Finn, R. D. (2012) The Pfam protein families database. *Nucleic Acids Res.* **40**, D290–D301
95. Tamura, K., Stecher, G., Peterson, D., Filipski, A., and Kumar, S. (2013) MEGA6: molecular evolutionary genetics analysis version 6.0. *Mol. Biol. Evol.* **30**, 2725–2729
96. Edgar, R. C. (2004) MUSCLE: multiple sequence alignment with high accuracy and high throughput. *Nucleic Acids Res.* **32**, 1792–1797